

CASE FILE
COPY

NASA TECHNICAL
MEMORANDUM



NASA TM X-1684

NASA TM X-1684

AERODYNAMIC CHARACTERISTICS
OF 0.25-SCALE MODEL OF
TOMAHAWK LAUNCH VEHICLE AT
MACH NUMBERS FROM 2.30 TO 4.63

by Lloyd S. Jernell

Langley Research Center

Langley Station, Hampton, Va.

AERODYNAMIC CHARACTERISTICS OF 0.25-SCALE MODEL OF
TOMAHAWK LAUNCH VEHICLE AT MACH NUMBERS

FROM 2.30 TO 4.63

By Lloyd S. Jernell

Langley Research Center
Langley Station, Hampton, Va.

NATIONAL AERONAUTICS AND SPACE ADMINISTRATION

For sale by the Clearinghouse for Federal Scientific and Technical Information
Springfield, Virginia 22151 – CFSTI price \$3.00

AERODYNAMIC CHARACTERISTICS OF 0.25-SCALE MODEL OF TOMAHAWK LAUNCH VEHICLE AT MACH NUMBERS

FROM 2.30 TO 4.63

By Lloyd S. Jernell
Langley Research Center

SUMMARY

An investigation of several configurations of a 0.25-scale model of the Tomahawk launch vehicle has been conducted in the Langley Unitary Plan wind tunnel at Mach numbers from 2.30 to 4.63. The investigation included the effects of body fineness ratio, fin planform geometry, and fin cant angle for an angle-of-attack range of about -4° to 21° at roll angles from 0° to 67° .

The results indicate that for the moment reference center employed, each configuration experienced pitch-up at angles of attack of approximately 8° to 10° at a Mach number of 2.30, with the angle of pitch-up decreasing with increasing Mach number. The larger fins delay pitch-up to a slightly higher angle of attack at all test Mach numbers. Canting the basic fins 1° was effective in producing rolling moment throughout the ranges of angle of attack and Mach number. Varying the roll angle resulted in large variations in the lateral force and moments above angles of attack of about 4° because of the effects of the forebody vortices acting on the fins.

INTRODUCTION

The Tomahawk launch vehicle, used in various flight-research projects by the National Aeronautics and Space Administration, is capable of boosting a variety of payloads to a Mach number of about 8. The estimated stability characteristics and the limited flight experience of the vehicle were considered inadequate for the assurance of successful flights for the various payload arrangements. Limited wind-tunnel tests have been conducted for several models of the vehicle but no data are available for Mach numbers from 2.4 to 5.0. Hence, an investigation was made in the Langley Unitary Plan wind tunnel to determine the static stability characteristics of a 0.25-scale model of the vehicle. The effects of body fineness ratio, fin planform geometry, and fin cant angle were investigated for Mach numbers from 2.30 to 4.63 at roll angles from 0° to 67° . The test Reynolds number was 2.5×10^6 per foot (8.2×10^6 per meter).

SYMBOLS

Data are presented about the nonrolling body system of axes. The moment reference center was located 17.44 inches (44.298 cm) forward of the model base.

| | |
|--------------------|---|
| A | body cross-sectional area, square feet (square meters) |
| C_A | axial-force coefficient, $\frac{\text{Axial force}}{qA}$ |
| C_l | rolling-moment coefficient, $\frac{\text{Rolling moment}}{qAd}$ |
| $C_{l\delta_f}$ | fin effectiveness parameter, $\frac{\Delta C_l}{\Delta \delta_f}$ |
| C_m | pitching-moment coefficient, $\frac{\text{Pitching moment}}{qAd}$ |
| $C_{m\alpha}$ | slope of pitching-moment curve at $\alpha \approx 0^\circ$, $\frac{\partial C_m}{\partial \alpha}$ |
| C_N | normal-force coefficient, $\frac{\text{Normal force}}{qA}$ |
| $C_{N\alpha}$ | slope of normal-force curve at $\alpha \approx 0^\circ$, $\frac{\partial C_N}{\partial \alpha}$ |
| C_n | yawing-moment coefficient, $\frac{\text{Yawing moment}}{qAd}$ |
| C_Y | side-force coefficient, $\frac{\text{Side force}}{qA}$ |
| d | body diameter, inches (centimeters) |
| l | length of each individual configuration, inches (centimeters) |
| M | free-stream Mach number |
| q | free-stream dynamic pressure, pounds per square foot (newtons per square meter) |
| $\frac{x_{ac}}{l}$ | position of aerodynamic center measured from nose |
| α | angle of attack, referenced to model center line, degrees |
| δ_f | fin cant angle, degrees |

ϕ roll angle, positive for model rolled to right, degrees

Model component identifications:

| | |
|----------------|---|
| B ₁ | afterbody |
| E ₁ | cylindrical extension, fineness ratio = 4.0 |
| E ₂ | cylindrical extension, fineness ratio = 6.0 |
| E ₃ | cylindrical extension, fineness ratio = 8.0 |
| F ₁ | basic fins, cant angle of 0° |
| F ₂ | basic fins, cant angle of 1° |
| F ₅ | large alternate fins |
| N ₁ | ogive nose, fineness ratio = 3.0 |

APPARATUS AND METHODS

Model

The 0.25-scale model, details of which are provided in figure 1, consisted of a cylindrical body with an ogive nose of fineness ratio of 3.0 and four truncated fins. The basic configuration had an overall fineness ratio of approximately 24.7. Other configurations investigated had body lengths with overall fineness ratios of approximately 22.7 and 26.7. Cant angles of 0° and 1° were provided for the basic fins, which are shown in figure 1(b). In addition, a set of larger fins having a 31-percent increase in planform area and a trailing-edge angle of 70° were tested for a cant angle of 0°. (See fig. 1(c).)

Tunnel

The investigation was conducted in the high Mach number test section of the Langley Unitary Plan wind tunnel, which is a variable-pressure, return-flow facility. The test section is 4 feet (1.22 meters) square and approximately 7 feet (2.13 meters) long. The nozzle leading to the test section is of the asymmetric sliding-block type which permits a continuous variation in Mach numbers from about 2.30 to 4.70.

Measurements, Corrections, and Tests

Aerodynamic forces and moments were measured by means of a sting-supported six-component electric strain-gage balance mounted within the body. The base pressure was measured by means of static-pressure orifices located at the model base. Boundary-layer transition strips approximately 0.06 inch (1.6 mm) wide were located 0.4 inch (10.2 mm) aft of the fin leading edges, measured in the streamwise direction, and 1.2 inches (30.5 mm) aft of the nose apex. These strips were composed of No. 50 carborundum grains embedded in a plastic adhesive.

The tests were conducted at Mach numbers of 2.30, 2.96, 3.95, and 4.63. The Reynolds number was 2.5×10^6 per foot (8.2×10^6 per meter). Data were obtained for an angle-of-attack range of about -4° to 21° at roll angles from 0° to 67° . The angles of attack were corrected for tunnel airflow misalignment and model support-system deflection under aerodynamic load. The axial-force coefficients have been adjusted to a condition of free-stream static pressure at the model base. The stagnation dewpoint was maintained below -30° F (239° K) to assure negligible condensation effects.

PRESENTATION OF RESULTS

The results of this investigation are presented as follows:

| | Figure |
|--|--------|
| Effect of body fineness ratio on longitudinal aerodynamic characteristics. $\phi = 0^\circ$ | 2 |
| Effect of fins on longitudinal aerodynamic characteristics. $\phi = 0^\circ$ | 3 |
| Summary of effects of body fineness ratio and fin planform geometry on longitudinal aerodynamic characteristics. $\alpha \approx 0^\circ$; $\phi = 0^\circ$ | 4 |
| Effect of fin cant angle on longitudinal aerodynamic characteristics. $\phi = 0^\circ$ | 5 |
| Effect of roll angle on longitudinal aerodynamic characteristics at $M = 2.30$ | 6 |
| Effect of roll angle on longitudinal aerodynamic characteristics at $M = 2.96$ | 7 |
| Effect of roll angle on longitudinal aerodynamic characteristics at $M = 3.95$ | 8 |
| Effect of roll angle on longitudinal aerodynamic characteristics at $M = 4.63$ | 9 |
| Effect of body fineness ratio on lateral aerodynamic characteristics. $\phi = 0^\circ$ | 10 |
| Effect of fins on lateral aerodynamic characteristics. $\phi = 0^\circ$ | 11 |

| | Figure |
|---|--------|
| Effect of fin cant angle on lateral aerodynamic characteristics. $\phi = 0^\circ$ | 12 |
| Summary of effect of fin cant angle on rolling-moment coefficient. $\Delta\delta_f = 1^\circ$ | 13 |
| Effect of roll angle on lateral aerodynamic characteristics at $M = 2.30$ | 14 |
| Effect of roll angle on lateral aerodynamic characteristics at $M = 2.96$ | 15 |
| Effect of roll angle on lateral aerodynamic characteristics at $M = 3.95$ | 16 |
| Effect of roll angle on lateral aerodynamic characteristics at $M = 4.63$ | 17 |

DISCUSSION

In order to expedite publication, the data are presented without detailed analysis. A few pertinent remarks concerning the aerodynamic characteristics are appropriate, however.

The effects of body fineness ratio on the longitudinal stability characteristics are shown in figure 2. Increasing the body fineness ratio results in moderate increases in pitching-moment coefficient for positive angles of attack at all test Mach numbers. For the moment reference center employed, each configuration experienced pitch-up at angles of attack of approximately 8° to 10° at $M = 2.30$, with the angle for pitch-up decreasing with increasing Mach number. The effects of body fineness ratio on the axial-force and normal-force coefficients are small.

The effects of fin geometry on the longitudinal characteristics are shown in figure 3. The basic fins (configuration F1) increase the longitudinal stability of the configuration $N_1E_2B_1$ considerably throughout the Mach number range. Increasing fin size (configuration F5) provides a further small increase in stability. The larger fins also delay pitch-up to a slightly higher angle of attack at all test Mach numbers.

The data of figures 2 and 3 are summarized in figure 4 for angles of attack near 0° . Throughout the test Mach number range increasing the body fineness ratio (configurations $N_1E_1B_1F_1$, $N_1E_2B_1F_1$, and $N_1E_3B_1F_1$) results in an increase in the slope of the pitching-moment curve C_{m_α} but has a negligible effect on the slope of the normal-force curve C_{N_α} . The aerodynamic-center location, presented in percent of the length of each individual configuration, is not affected by body fineness ratio. The addition of the larger fins provides a slight rearward shift of the aerodynamic center at all test Mach numbers. Without fins, the aerodynamic center of the model is positioned considerably forward of the moment reference center, particularly at the higher Mach numbers.

Neither fin cant angle (fig. 5) nor model roll attitude (figs. 6 to 9) have any appreciable effect on the longitudinal aerodynamic characteristics.

Increasing the body fineness ratio generally reduces the induced rolling-moment variation with angle of attack at $M = 2.30$, but the effect diminishes with increasing Mach

number (fig. 10). Fin size has relatively little effect on the lateral aerodynamic characteristics (fig. 11). Canting the basic fins 1° is effective in producing a positive rolling-moment coefficient throughout the ranges of angle of attack and Mach number (fig. 12). The data of figure 12 are summarized in figure 13 in terms of fin cant-angle effectiveness on rolling-moment coefficient $C_{l\delta_f}$ plotted against Mach number for angles of attack from 0° to 20° . At $M = 2.30$, the rolling moment due to cant angle is maintained throughout the angle-of-attack range. At angles of attack to about 10° , there is approximately a 50-percent loss in the canting effect as Mach number increases to 4.63. However, at $\alpha = 20^\circ$ there is little effect of Mach number on $C_{l\delta_f}$. The increase in $C_{l\delta_f}$ with angle of attack at the higher Mach numbers is believed to be due to the increased local dynamic pressure in the region of the lower and horizontal fins.

At $M = 2.30$ changing the model roll attitude leads to large variations in the lateral coefficients at angles of attack greater than about 4° (fig. 14). The data of figures 14 to 17 show that these variations diminish significantly with an increase in Mach number. These effects, which are believed to be related to the relative position of the fins with respect to the vortices shedding from the nose, are discussed in references 1 and 2.

SUMMARY OF RESULTS

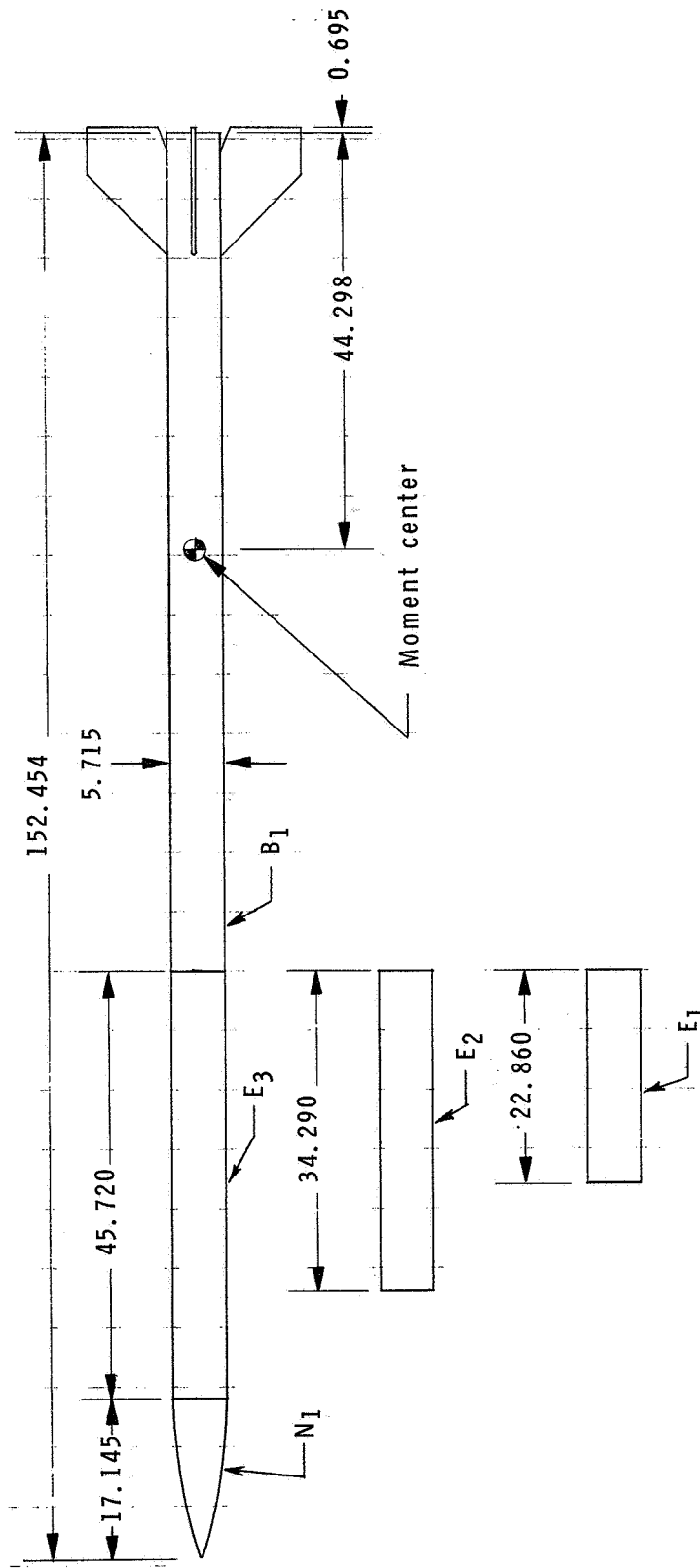
An investigation has been conducted to determine the effects of body fineness ratio, fin planform geometry, and fin cant angle on the longitudinal and lateral aerodynamic characteristics of a 0.25-scale model of the Tomahawk launch vehicle at Mach numbers from 2.30 to 4.63. The conclusions are summarized as follows:

1. For the moment reference center employed, each configuration experienced pitch-up at angles of attack of approximately 8° to 10° at a Mach number of 2.30, with the angle of pitch-up decreasing with increasing Mach number. The larger fins delay pitch-up to a slightly higher angle of attack at all test Mach numbers.
2. Canting the basic fins 1° was effective in producing rolling moment throughout the ranges of angle of attack and Mach number.
3. Varying the roll angle resulted in large variations in the lateral force and moments above angles of attack of about 4° because of the effects of forebody vortices acting on the fins.

Langley Research Center,
National Aeronautics and Space Administration,
Langley Station, Hampton, Va., August 16, 1968,
124-07-05-01-23.

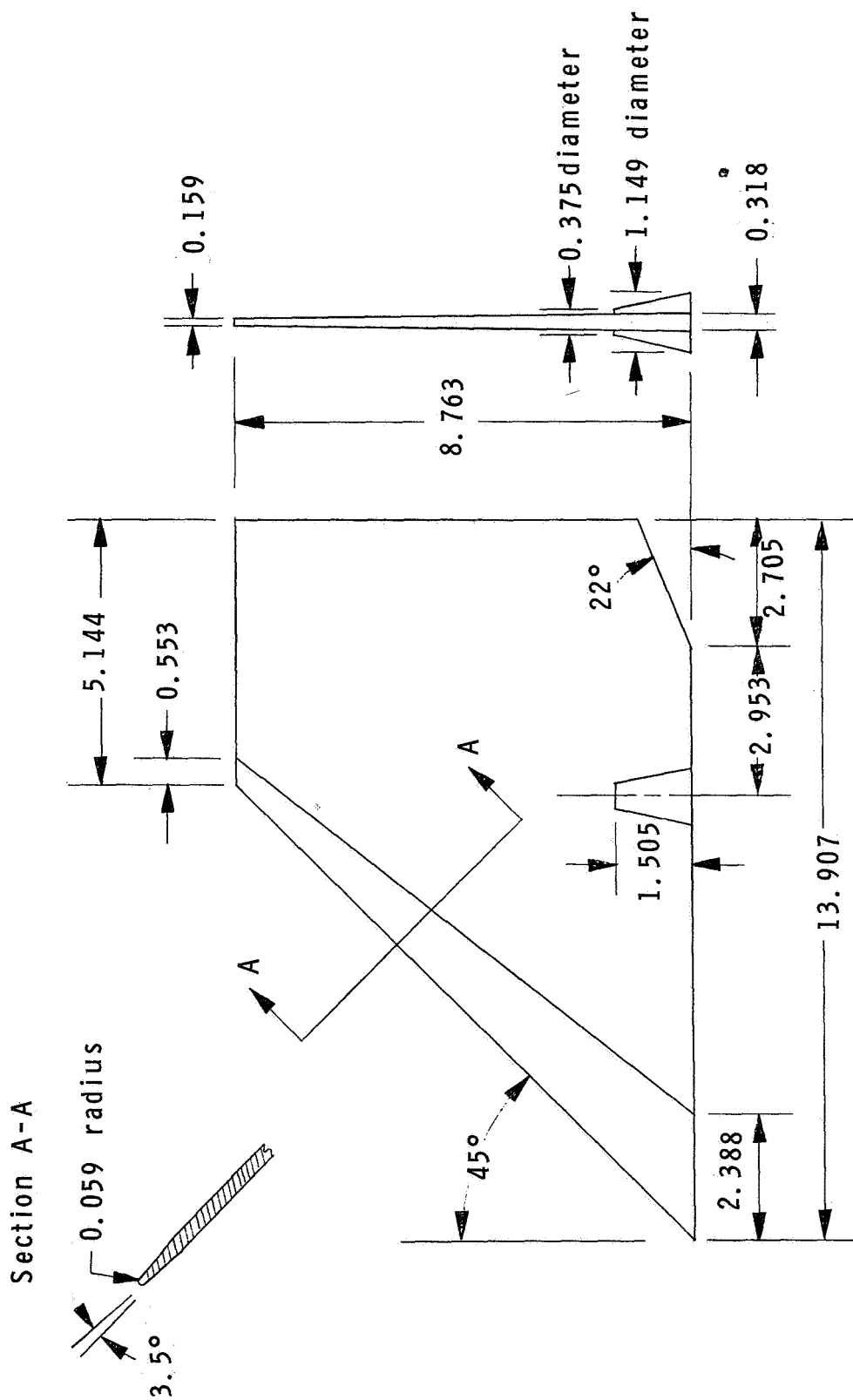
REFERENCES

1. Raney, D. J.: Measurement of the Cross Flow Around an Inclined Body at a Mach Number of 1.91. Tech. Note No. Aero 2357, Brit. R.A.E., Jan. 1955.
2. Ferris, James C.: Static Stability Investigation of a Single-Stage Sounding Rocket at Mach Numbers From 0.60 to 1.20. NASA TN D-4013, 1967.



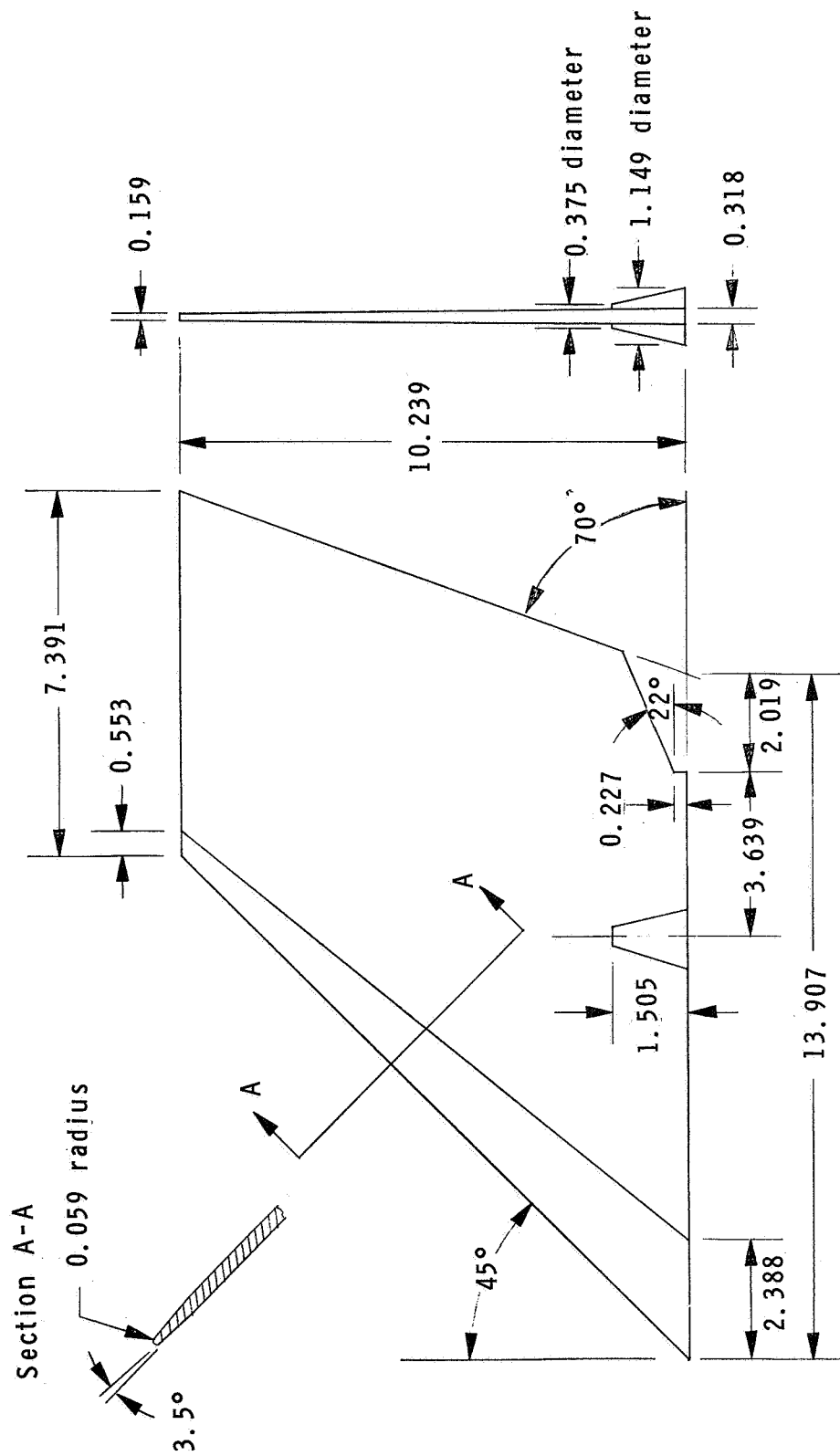
(a) Model geometry.

Figure 1.- Drawings of 0.25-scale model of Tomahawk vehicle. (Linear dimensions are in centimeters.)



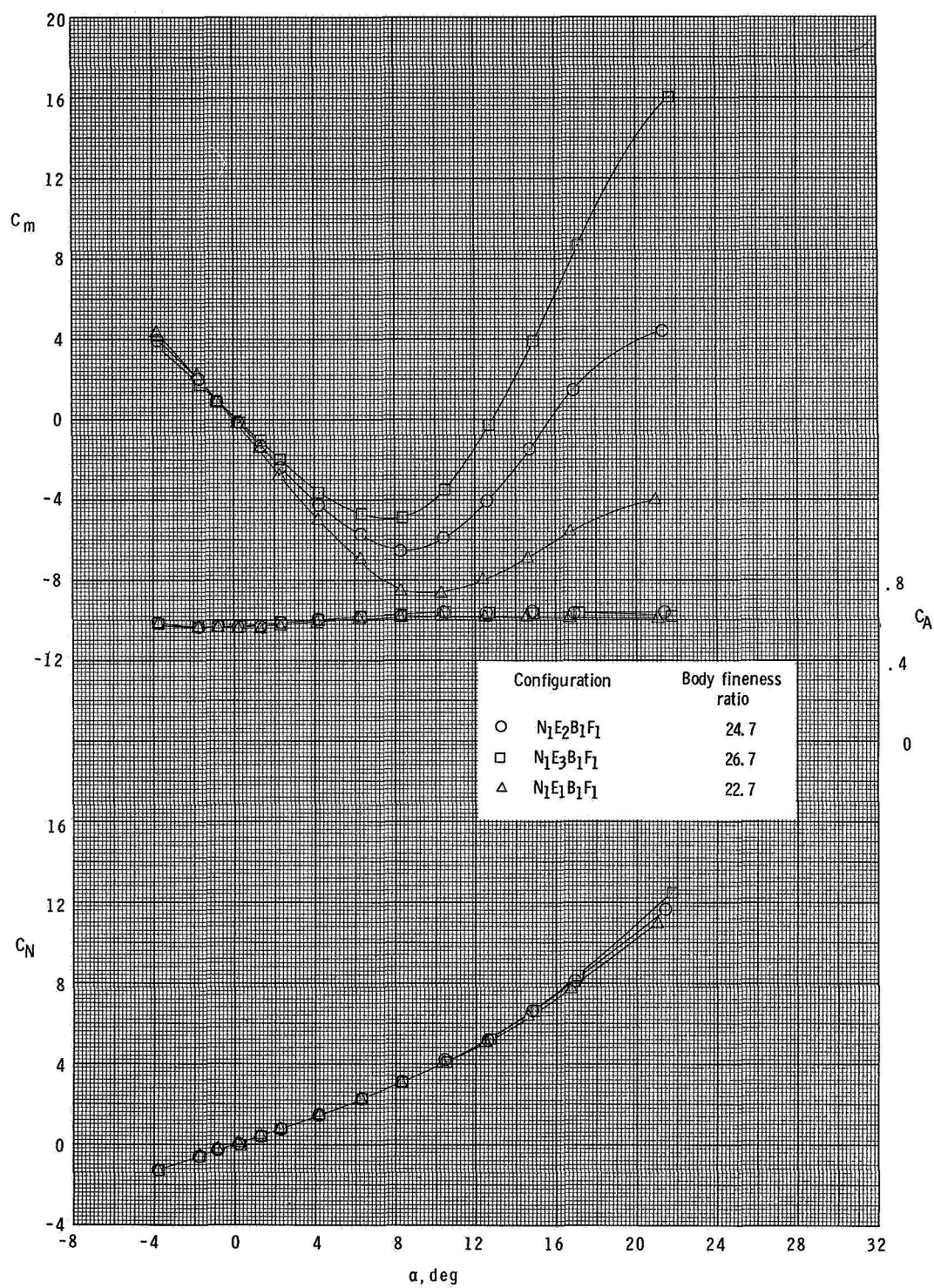
(b) Details of basic fins.

Figure 1.- Continued.



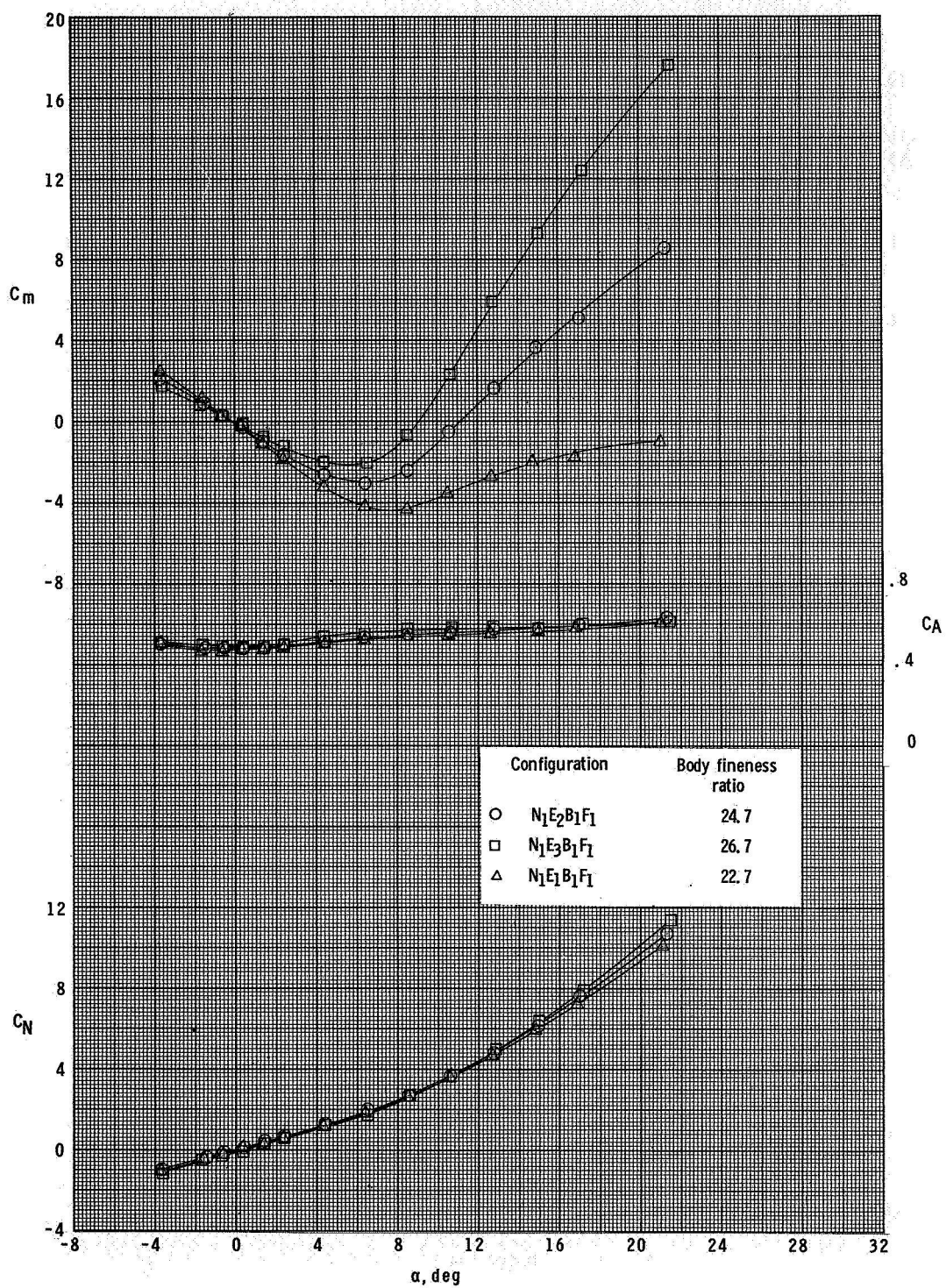
(c) Details of alternate fins.

Figure 1.- Concluded.



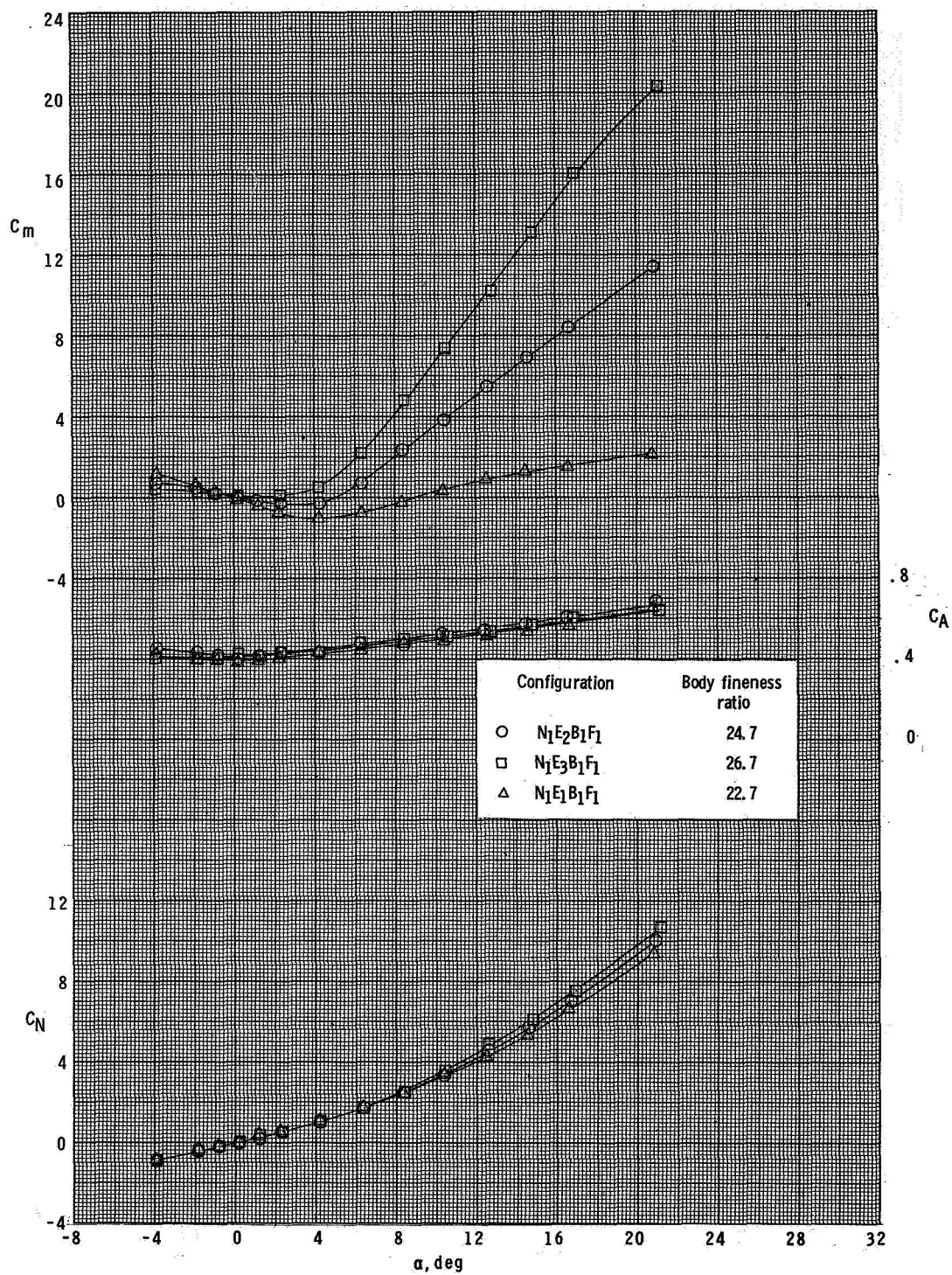
(a) $M = 2.30$.

Figure 2.- Effect of body fineness ratio on longitudinal aerodynamic characteristics. $\phi = 0^\circ$.



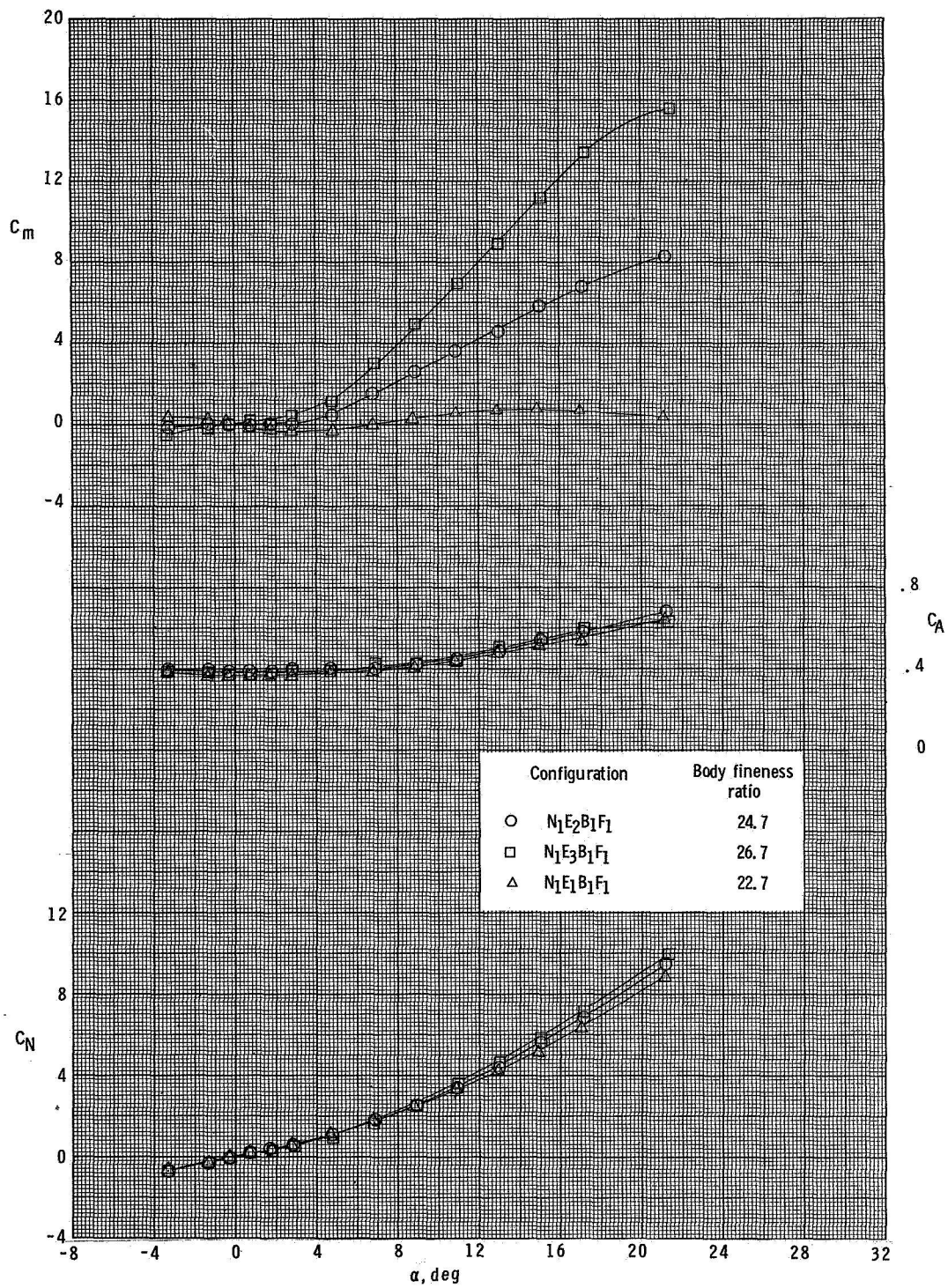
(b) $M = 2.96$.

Figure 2.- Continued.



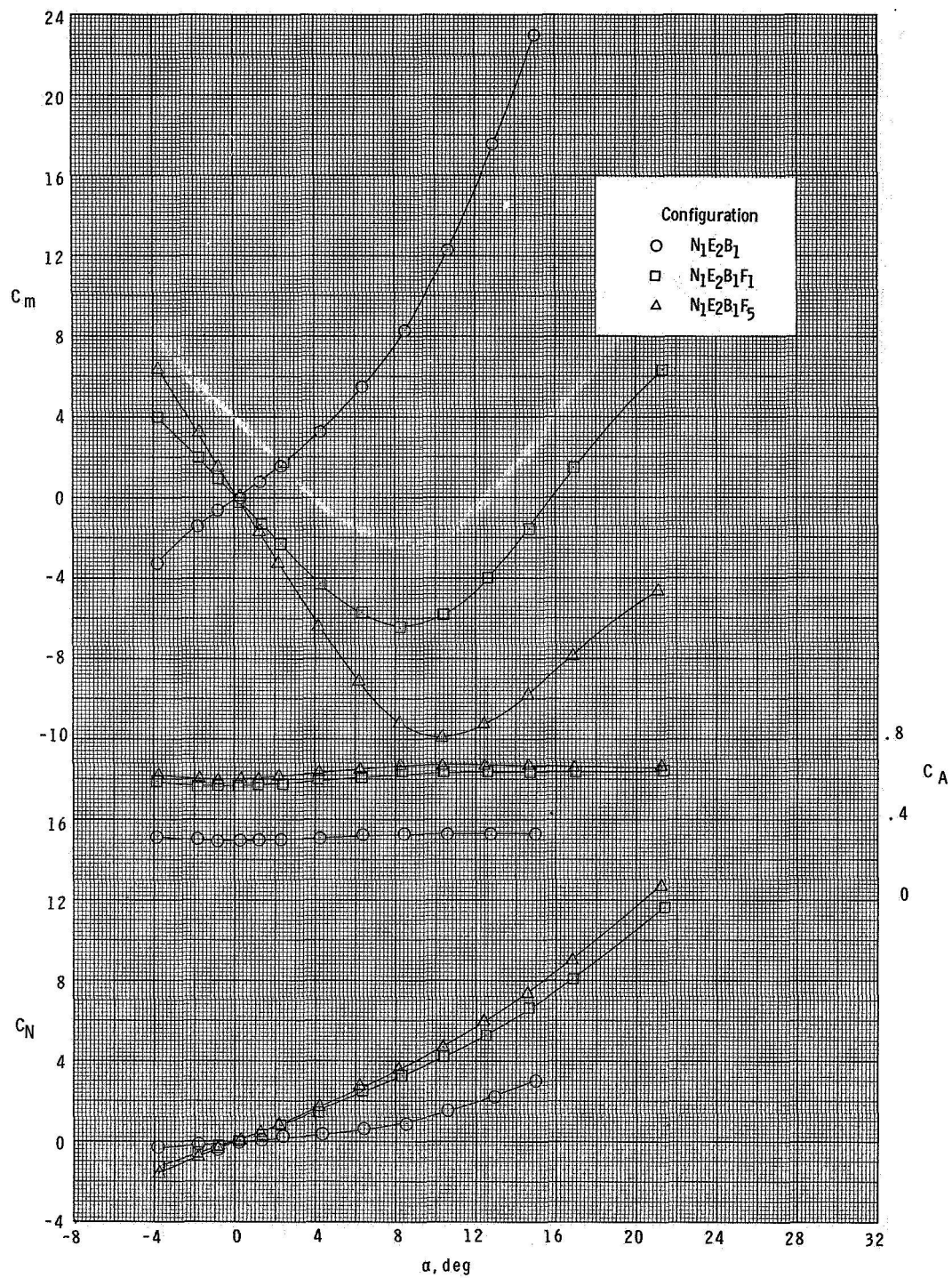
(c) $M = 3.95$.

Figure 2.- Continued.



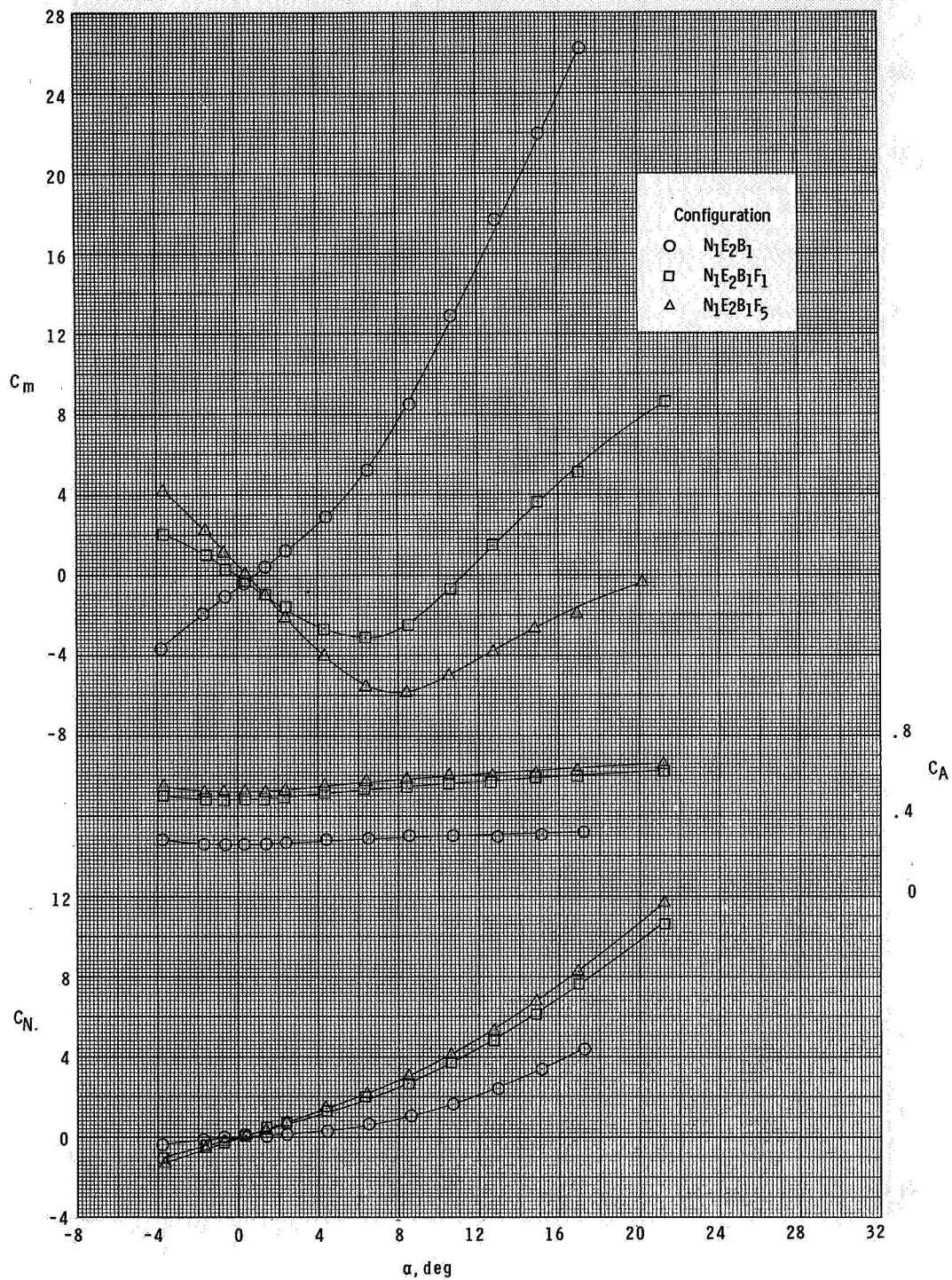
(d) $M = 4.63$.

Figure 2.- Concluded.



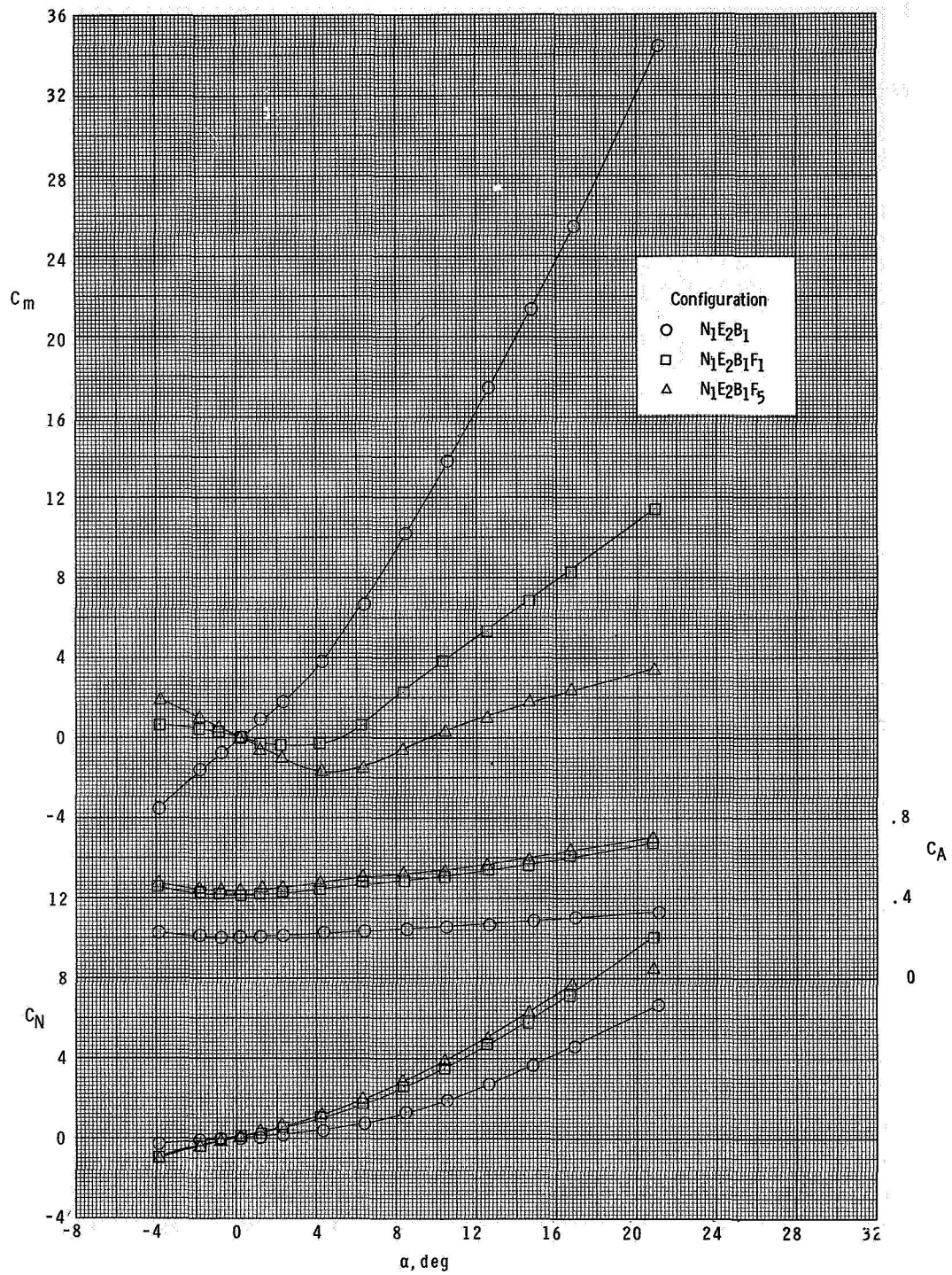
(a) $M = 2.30$.

Figure 3.- Effect of fins on longitudinal aerodynamic characteristics, $\phi = 0^\circ$.



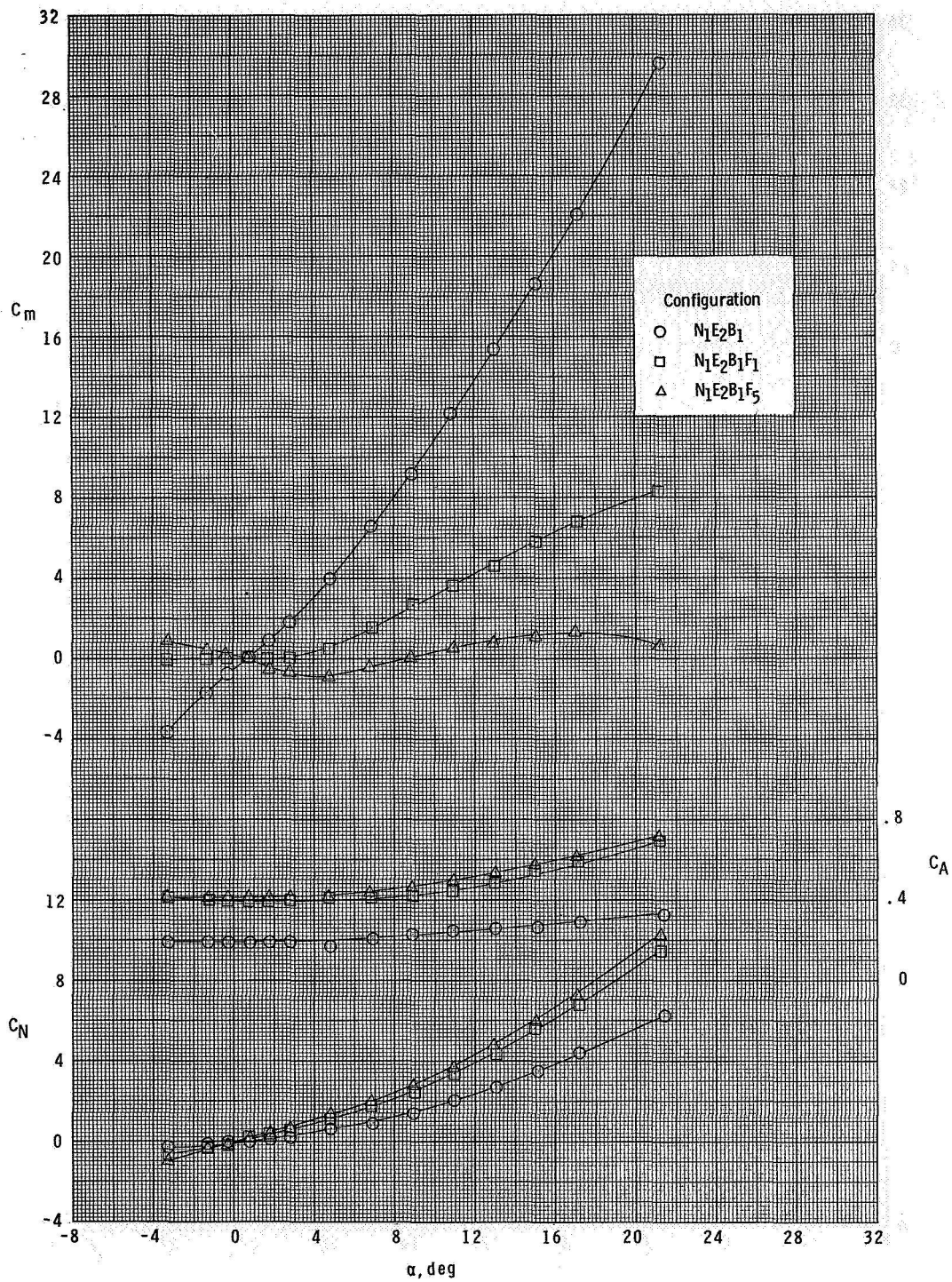
(b) $M = 2.96$.

Figure 3.- Continued.



(c) $M = 3.95$.

Figure 3.- Continued.



(d) $M = 4.63$.

Figure 3.- Concluded.

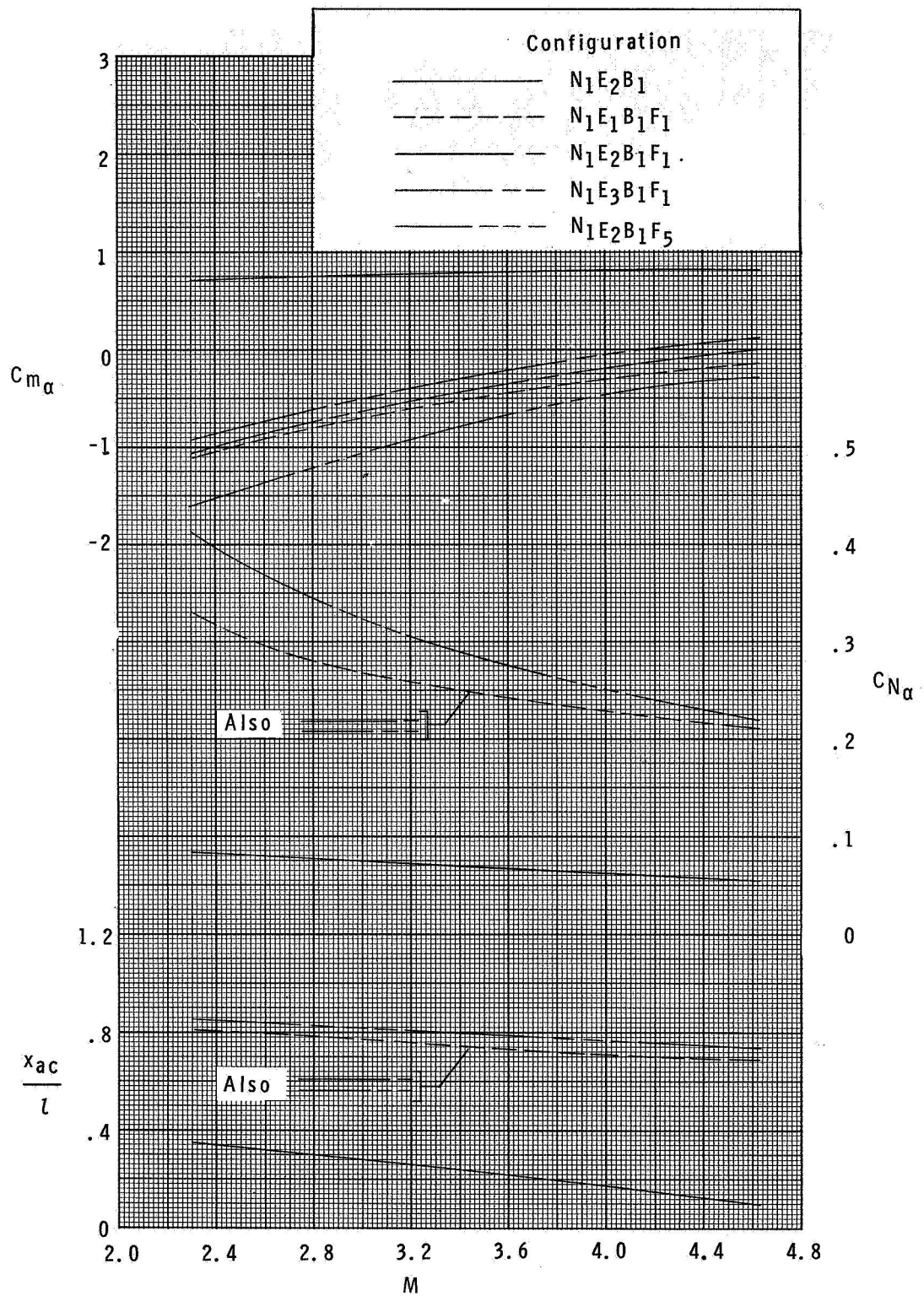
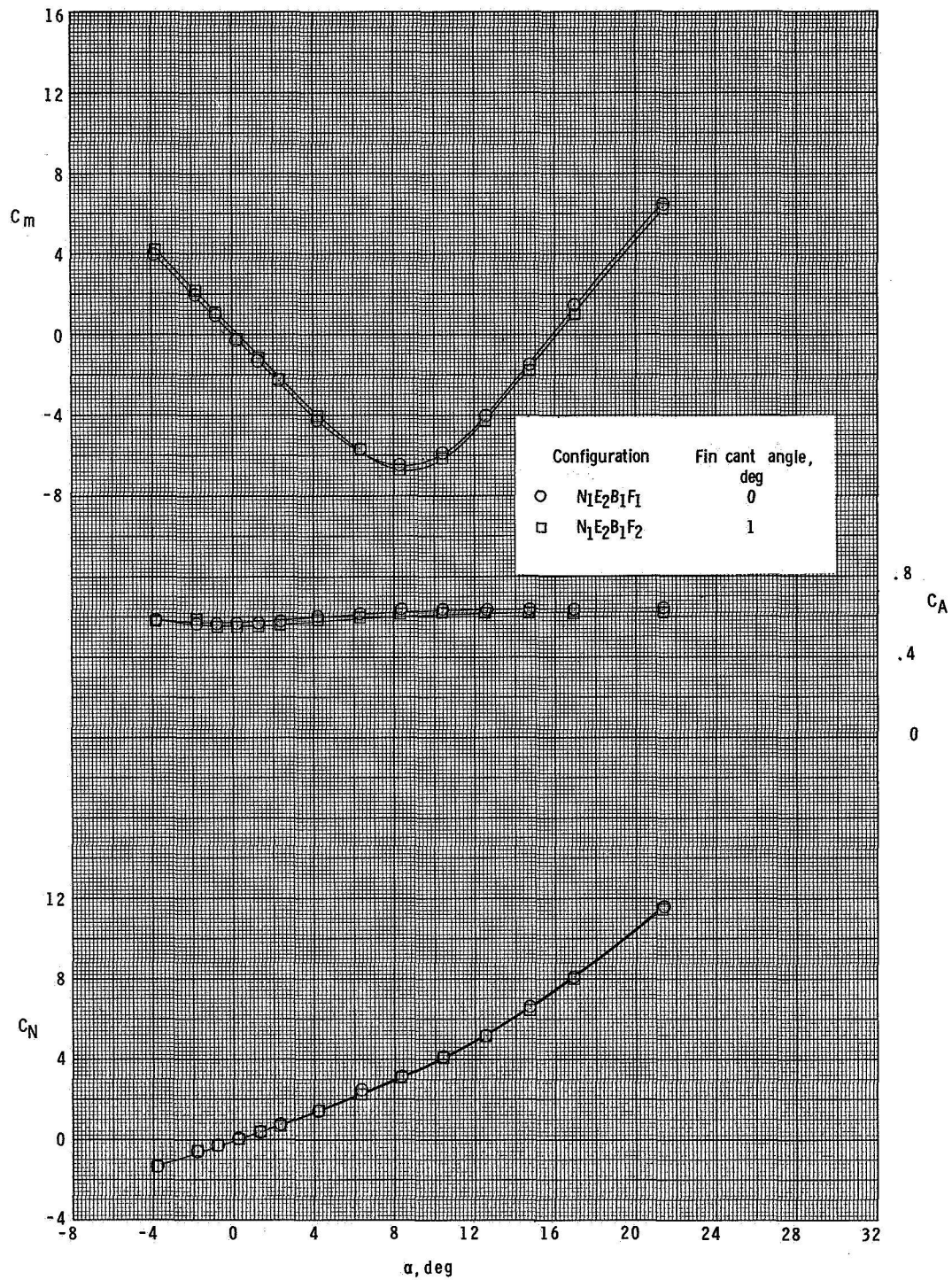
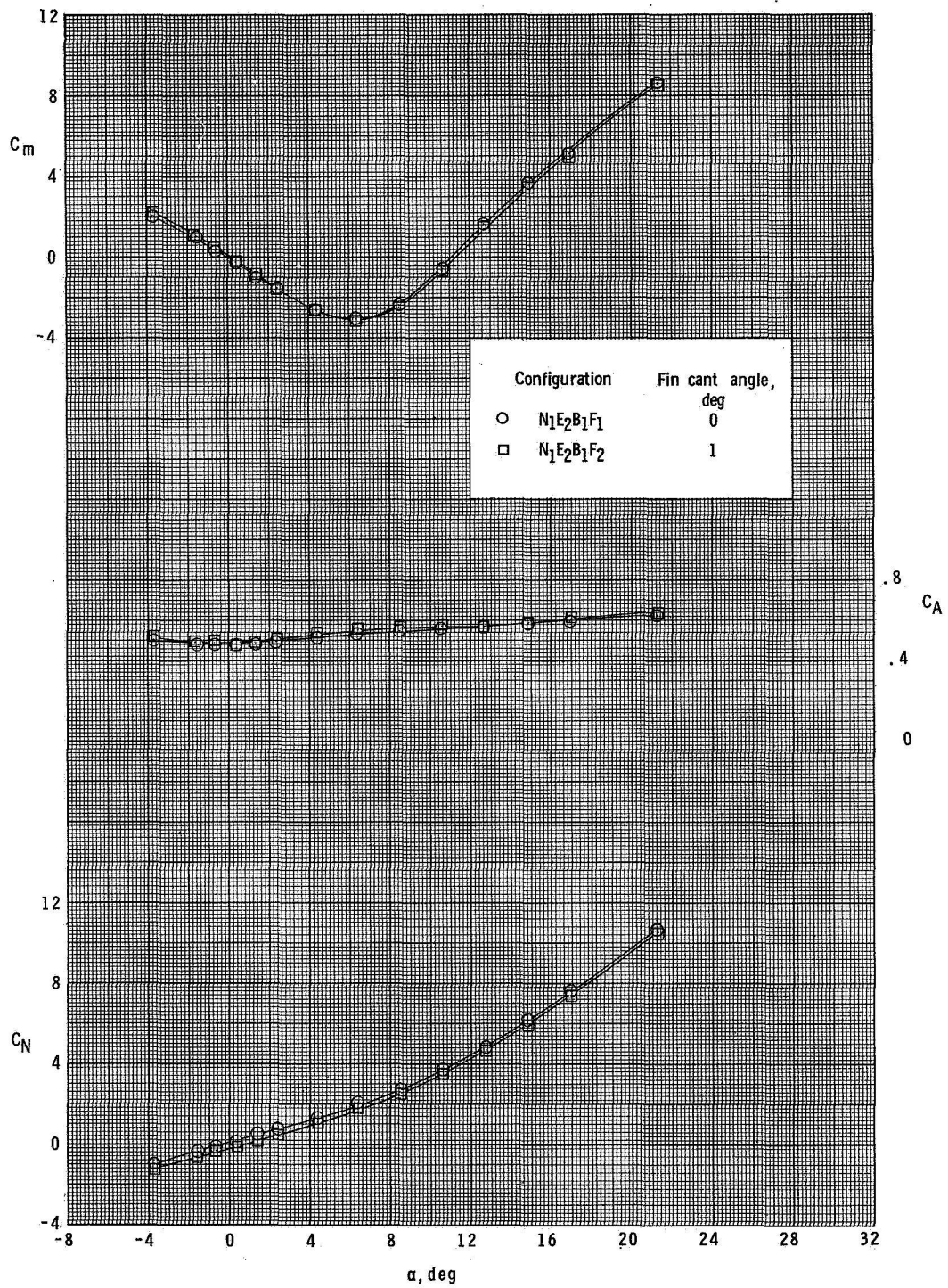


Figure 4.- Summary of effects of body fineness ratio and fin planform geometry on longitudinal aerodynamic characteristics.
 $\alpha \approx 0^\circ$; $\phi = 0^\circ$.



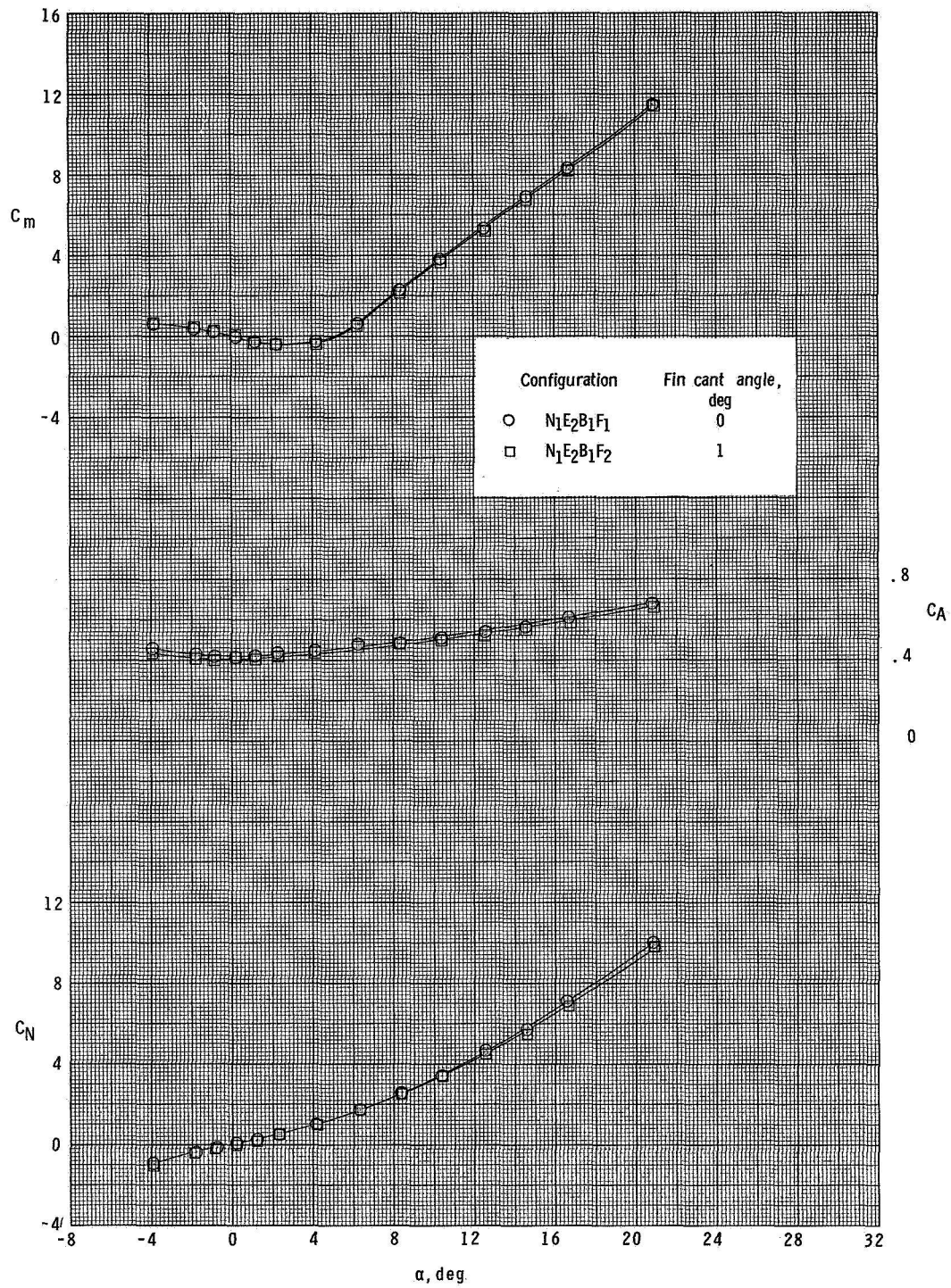
(a) $M = 2.30$.

Figure 5.- Effect of fin cant angle on longitudinal aerodynamic characteristics. $\phi = 0^\circ$.



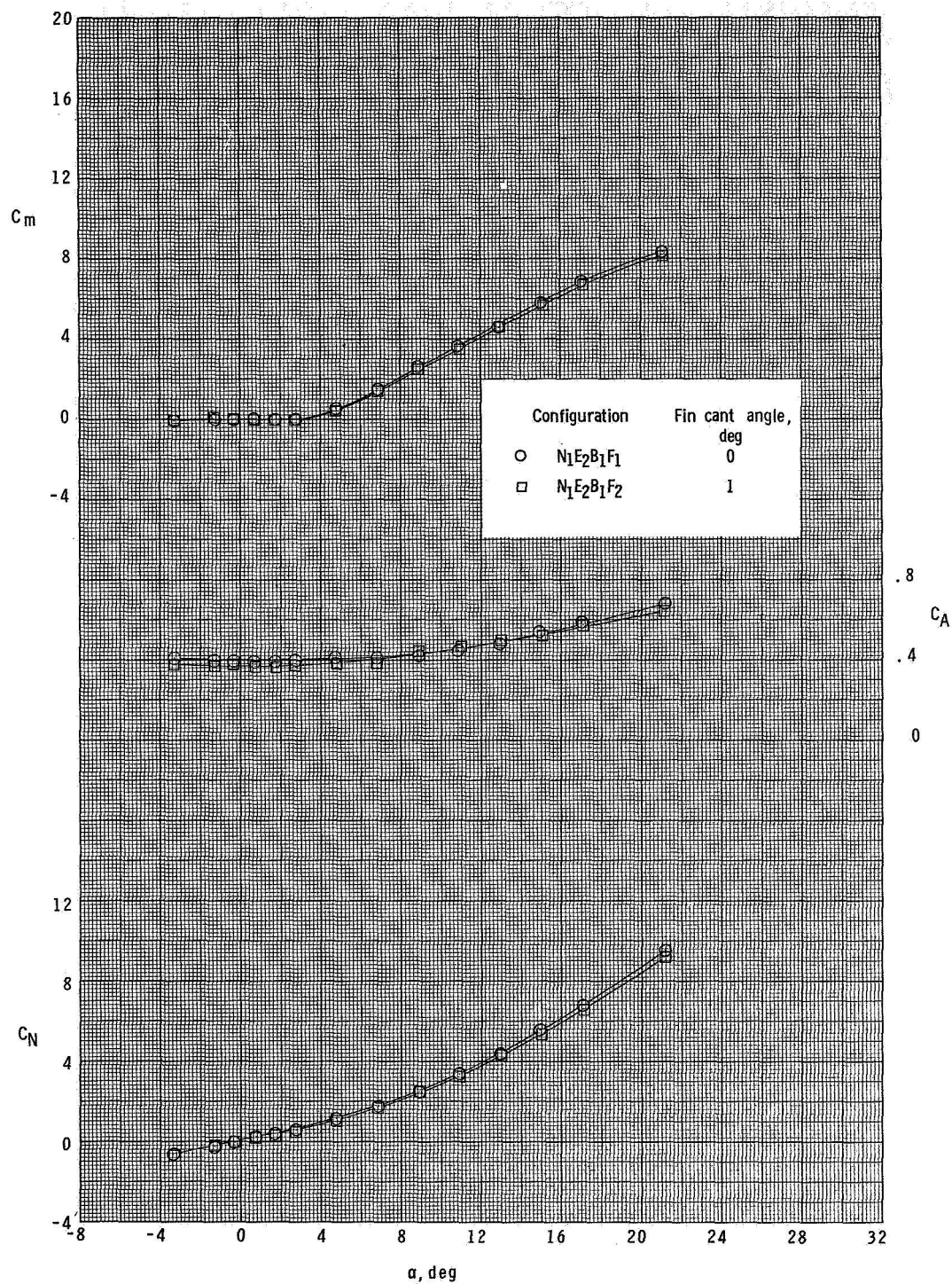
(b) $M = 2.96$.

Figure 5.- Continued.



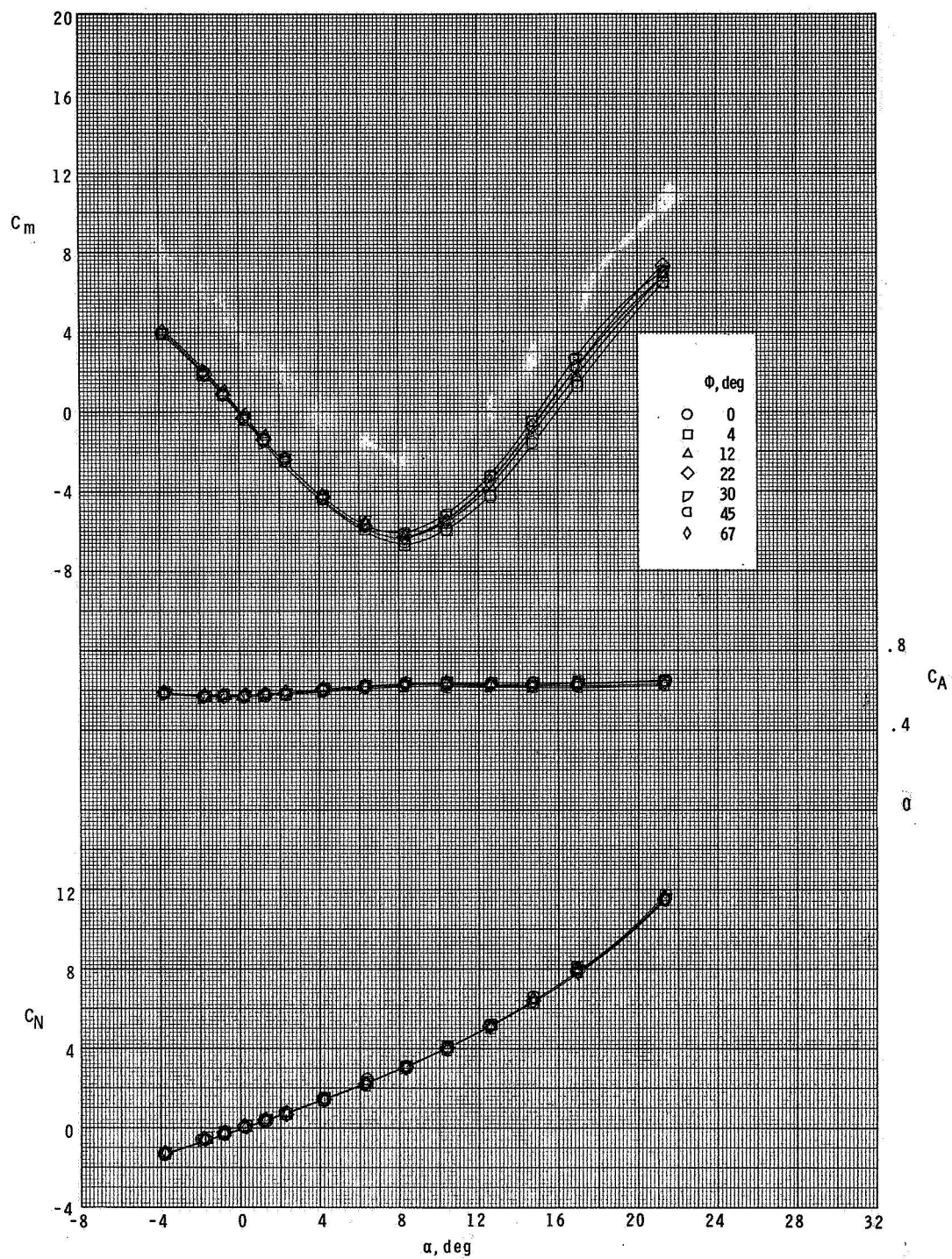
(c) $M = 3.95$.

Figure 5.- Continued.



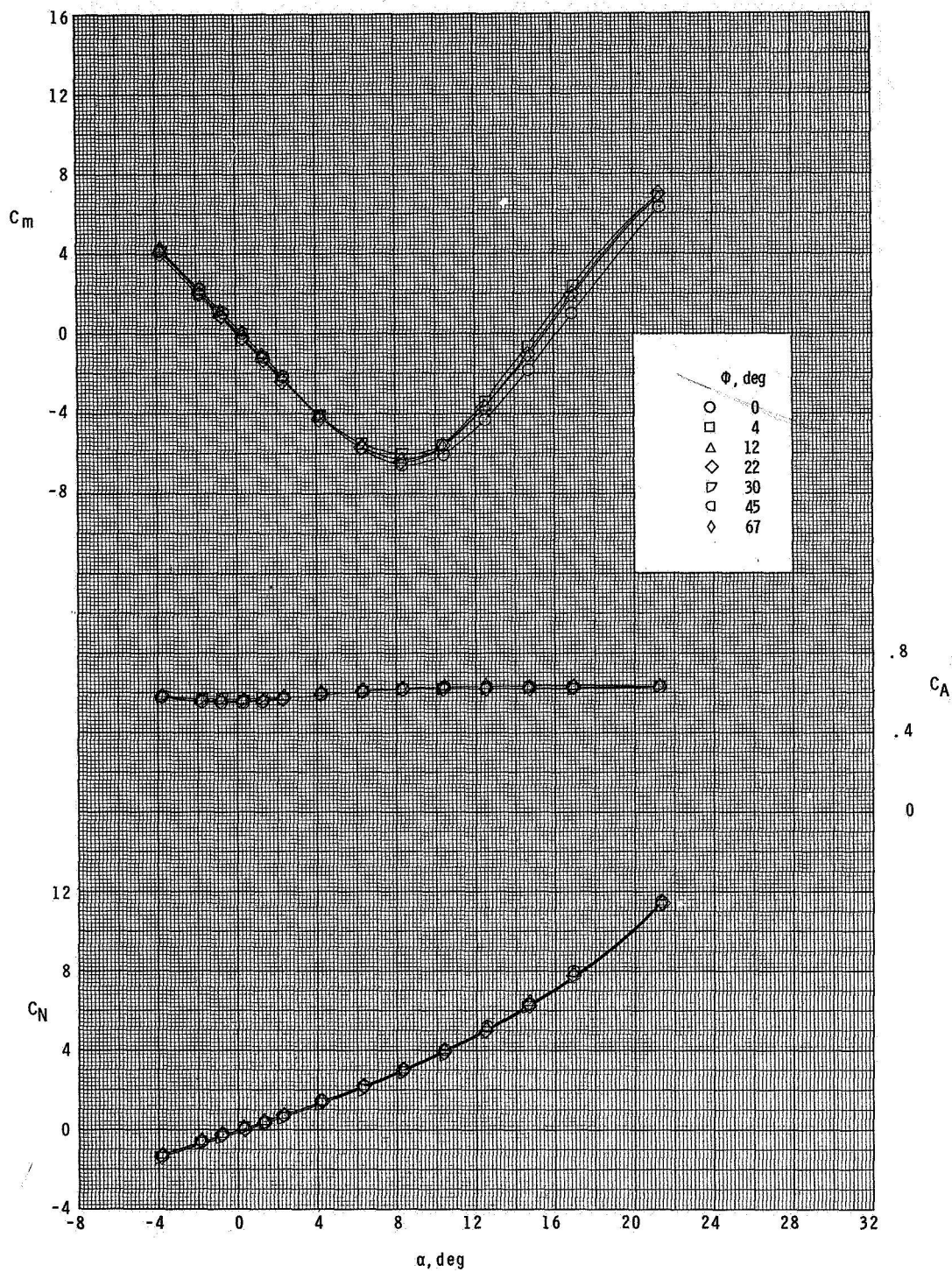
(d) $M = 4.63$.

Figure 5.- Concluded.



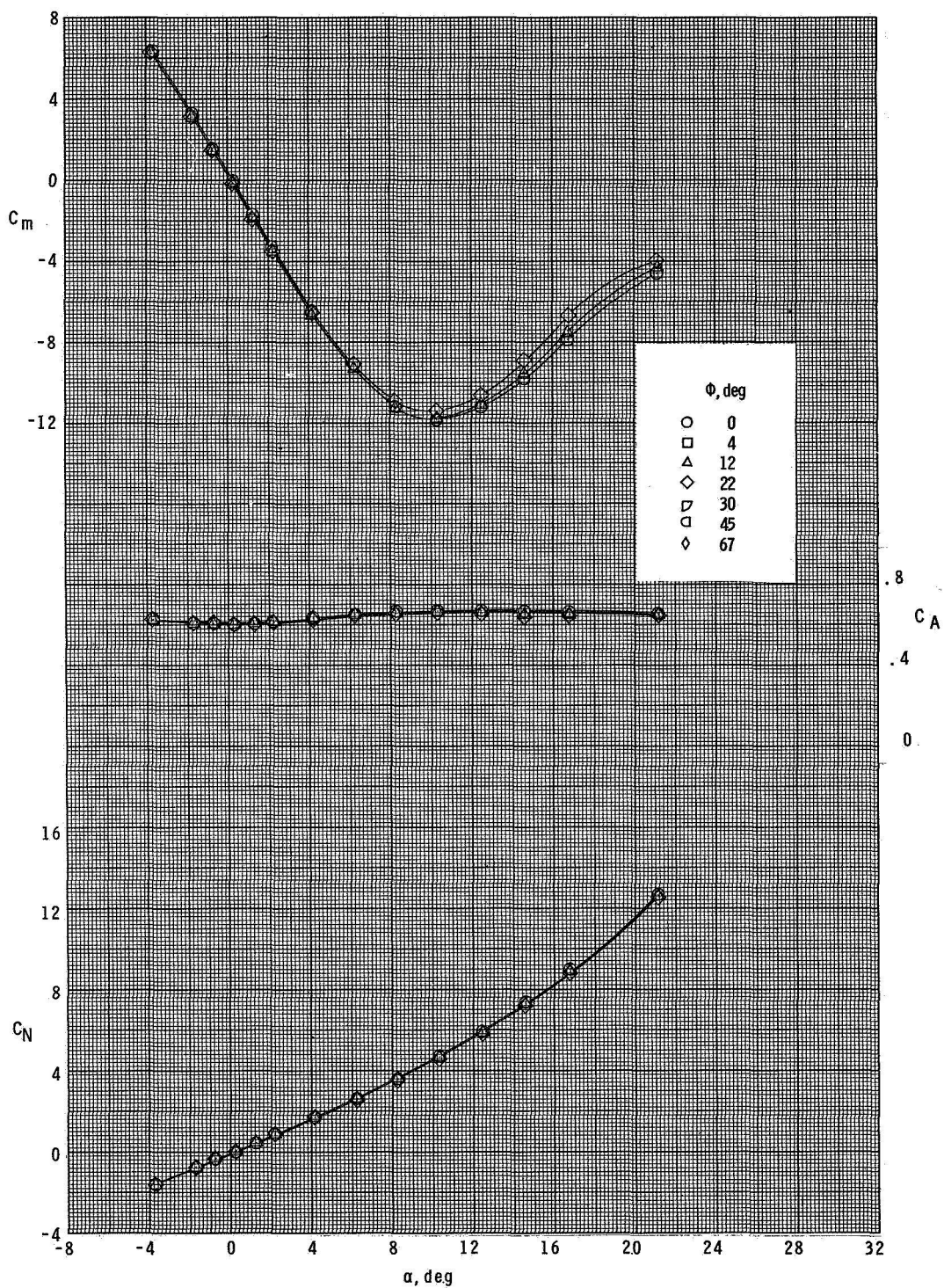
(a) Configuration $N_1E_2B_1F_1$.

Figure 6.- Effect of roll angle on longitudinal aerodynamic characteristics at $M = 2.30$.



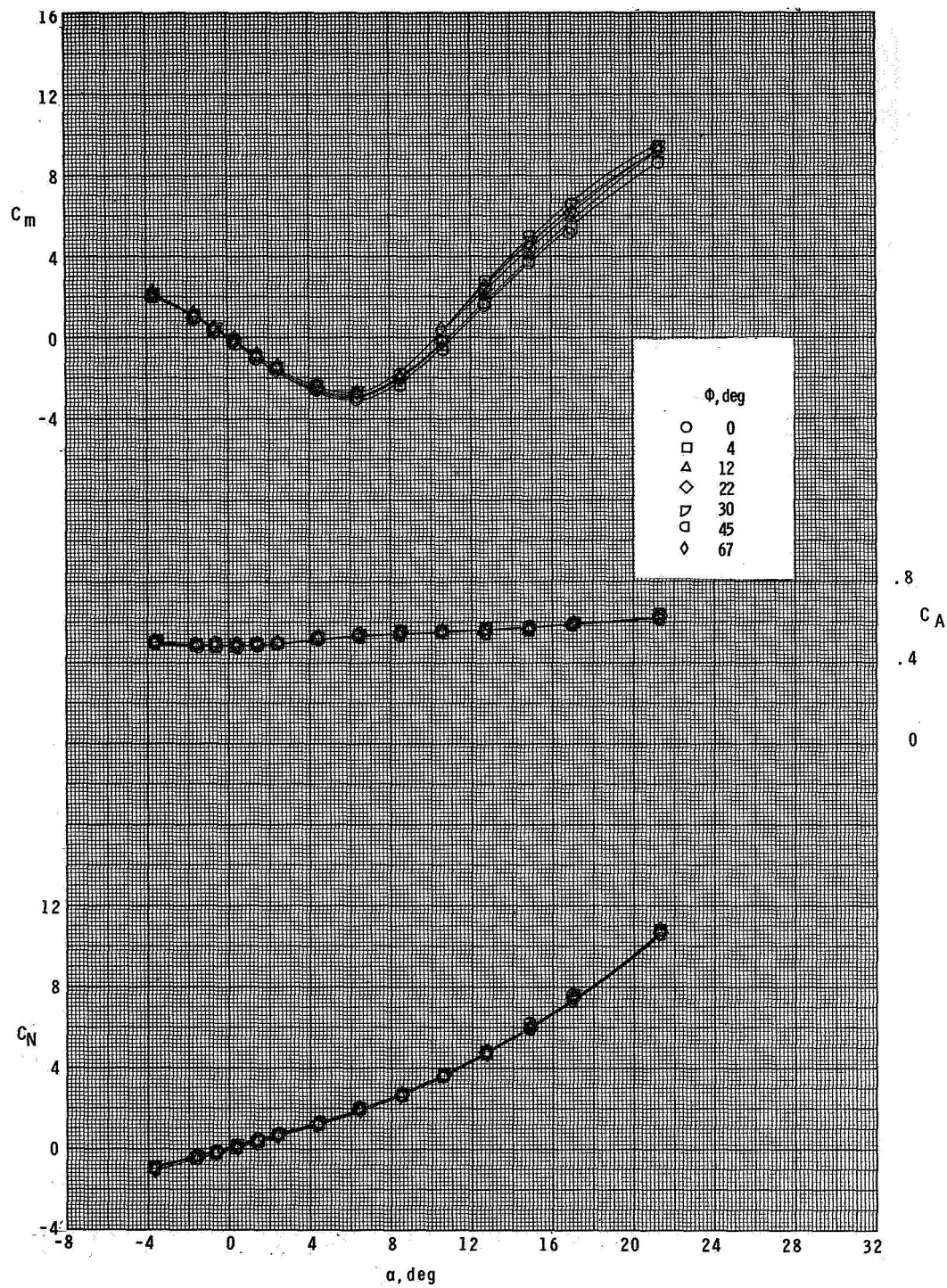
(b) Configuration $N_1E_2B_1F_2$.

Figure 6.- Continued.



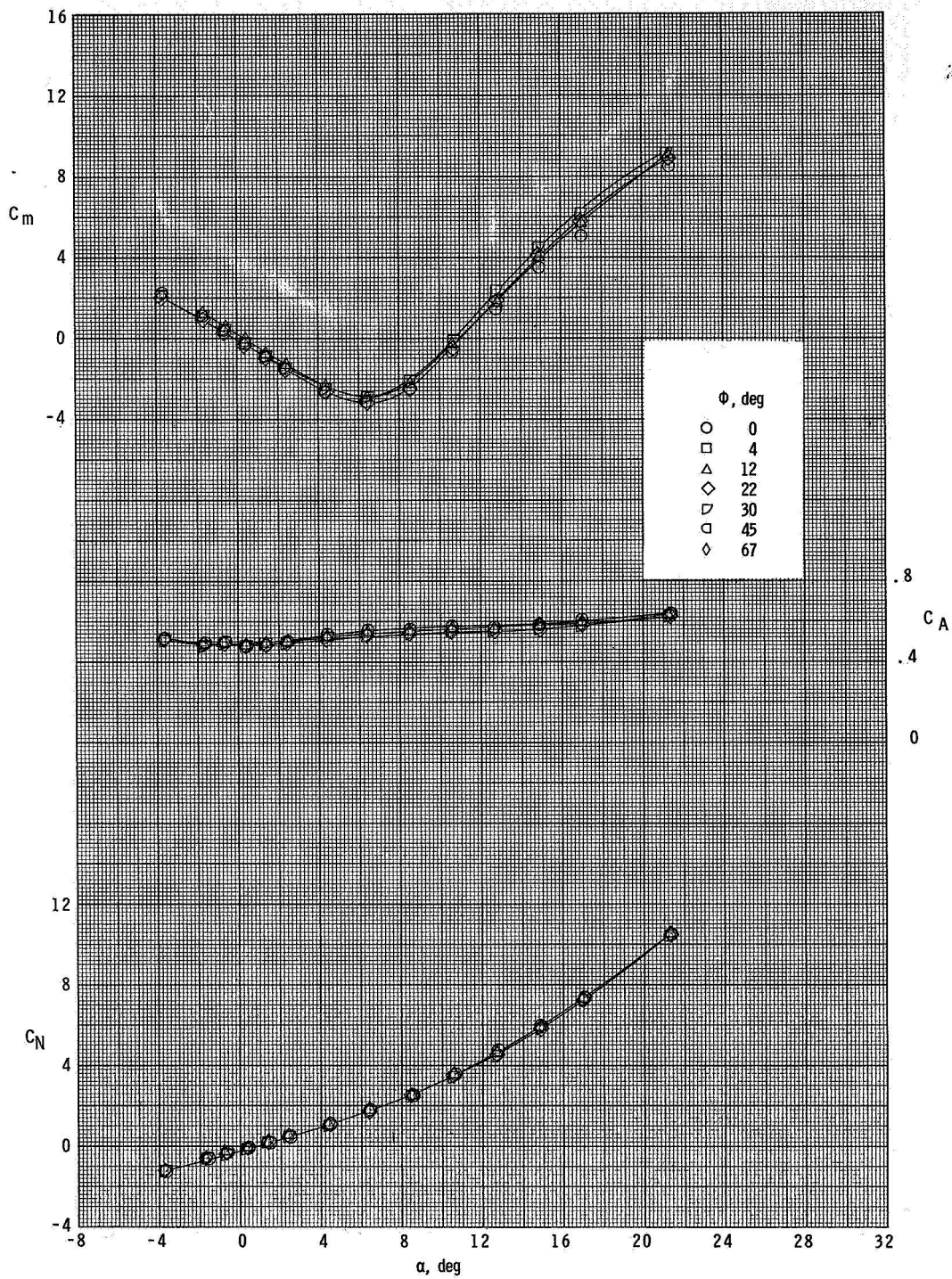
(c) Configuration $N_1E_2B_1F_5$.

Figure 6.- Concluded.



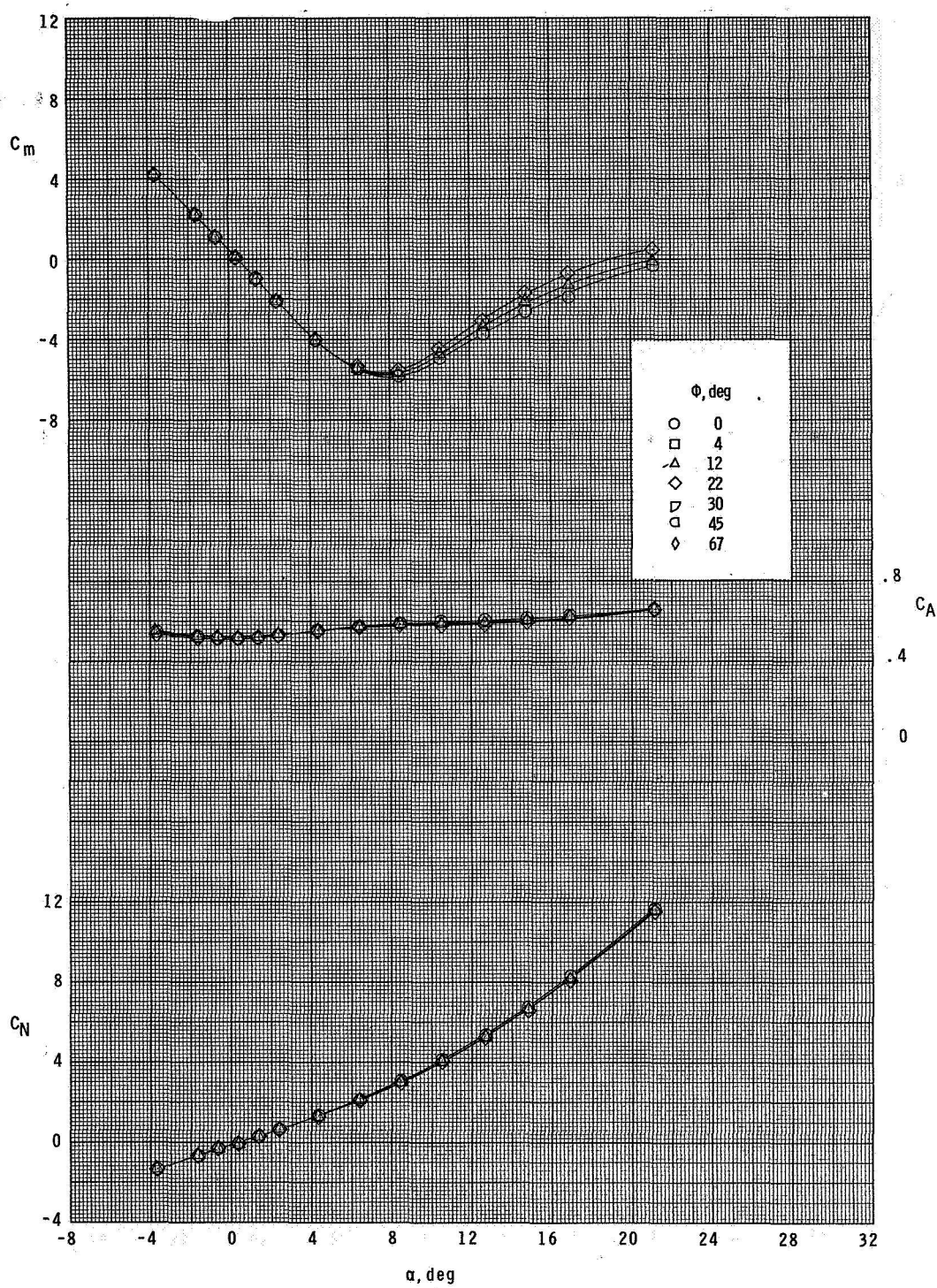
(a) Configuration $N_1E_2B_1F_1$.

Figure 7.- Effect of roll angle on longitudinal aerodynamic characteristics at $M = 2.96$.



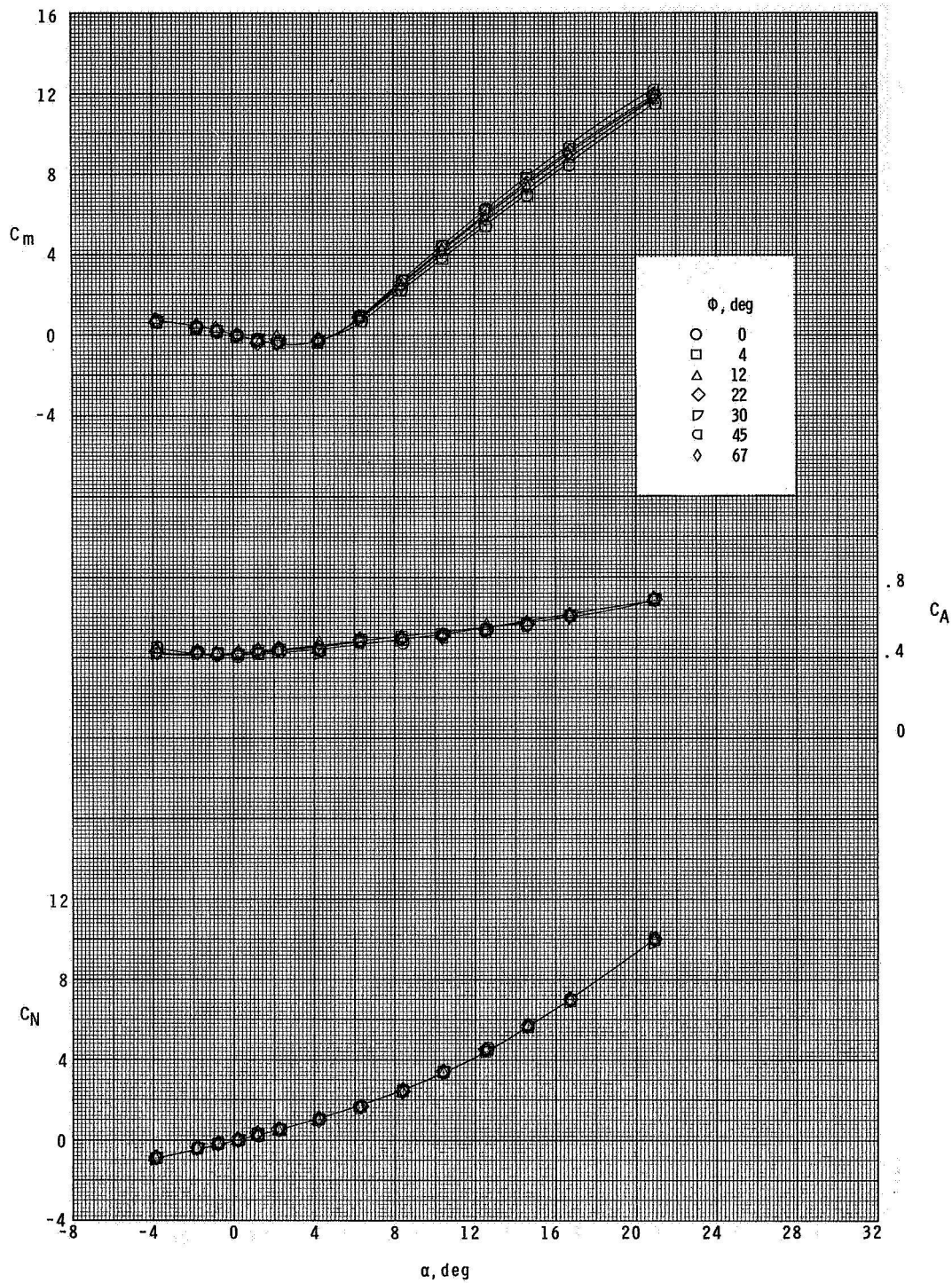
(b) Configuration $N_1E_2B_1F_2$.

Figure 7.- Continued.



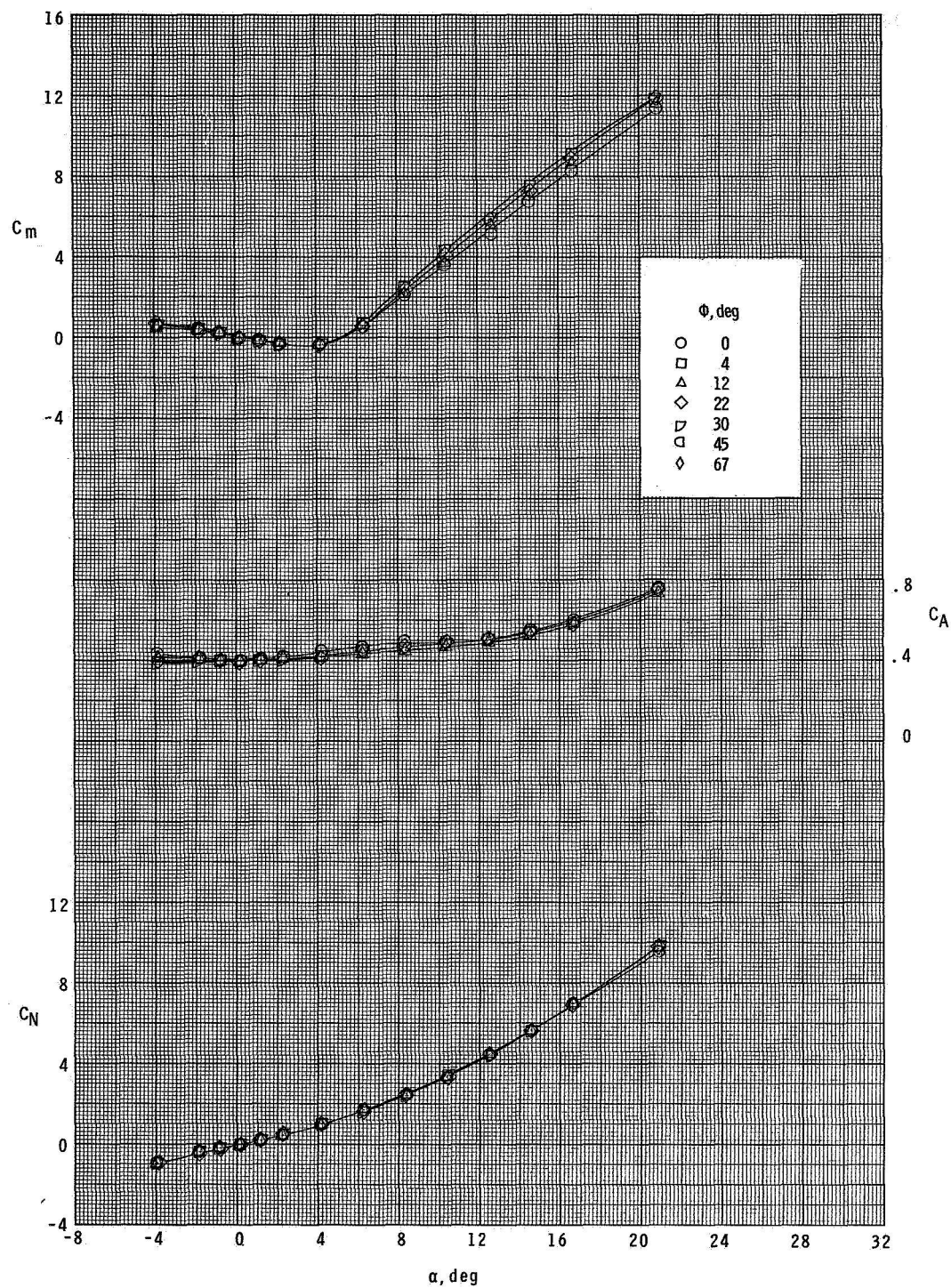
(c) Configuration $N_1E_2B_1F_5$

Figure 7.- Concluded.



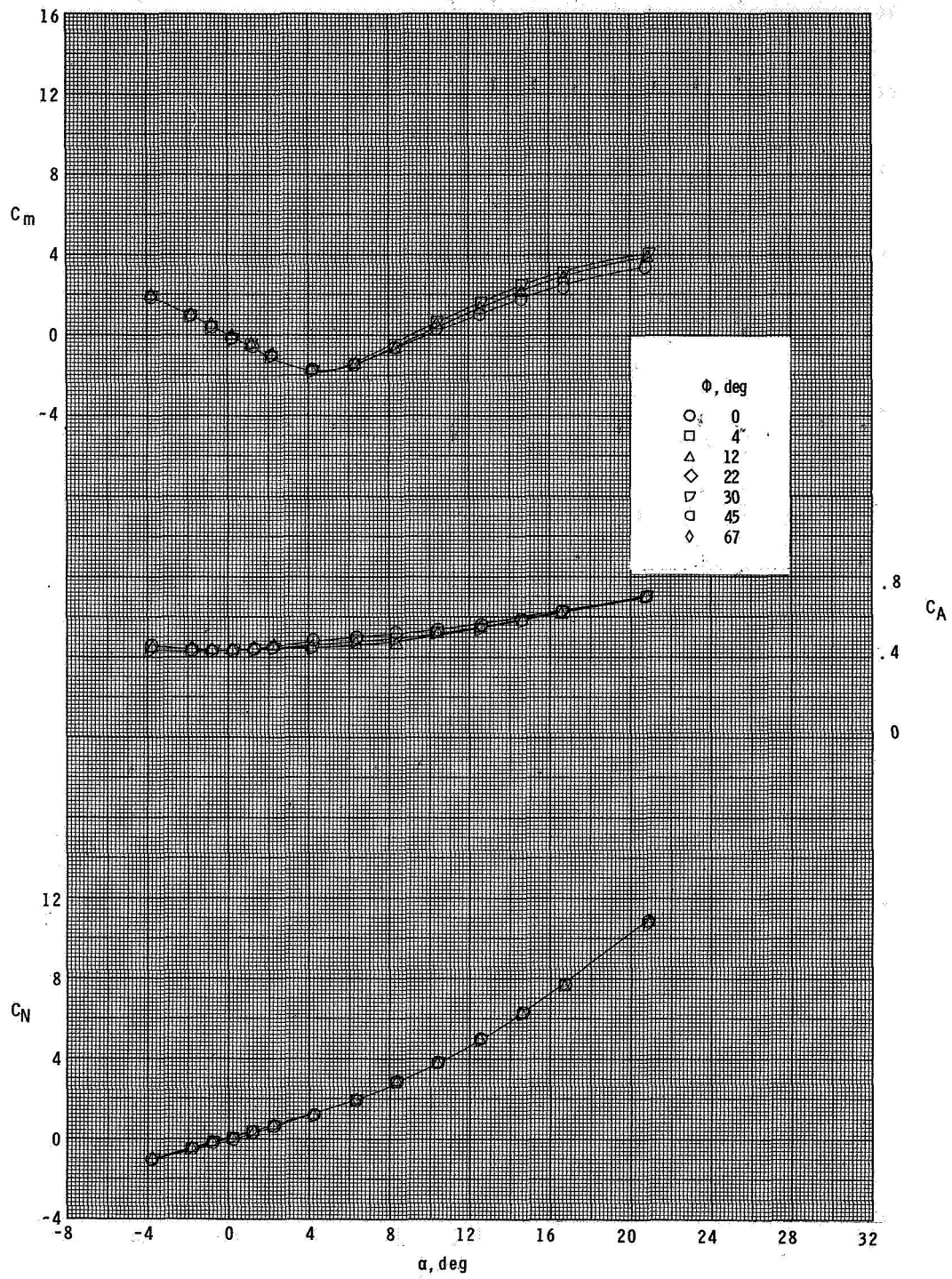
(a) Configuration $N_1E_2B_1F_1$.

Figure 8.- Effect of roll angle on longitudinal aerodynamic characteristics at $M = 3.95$.



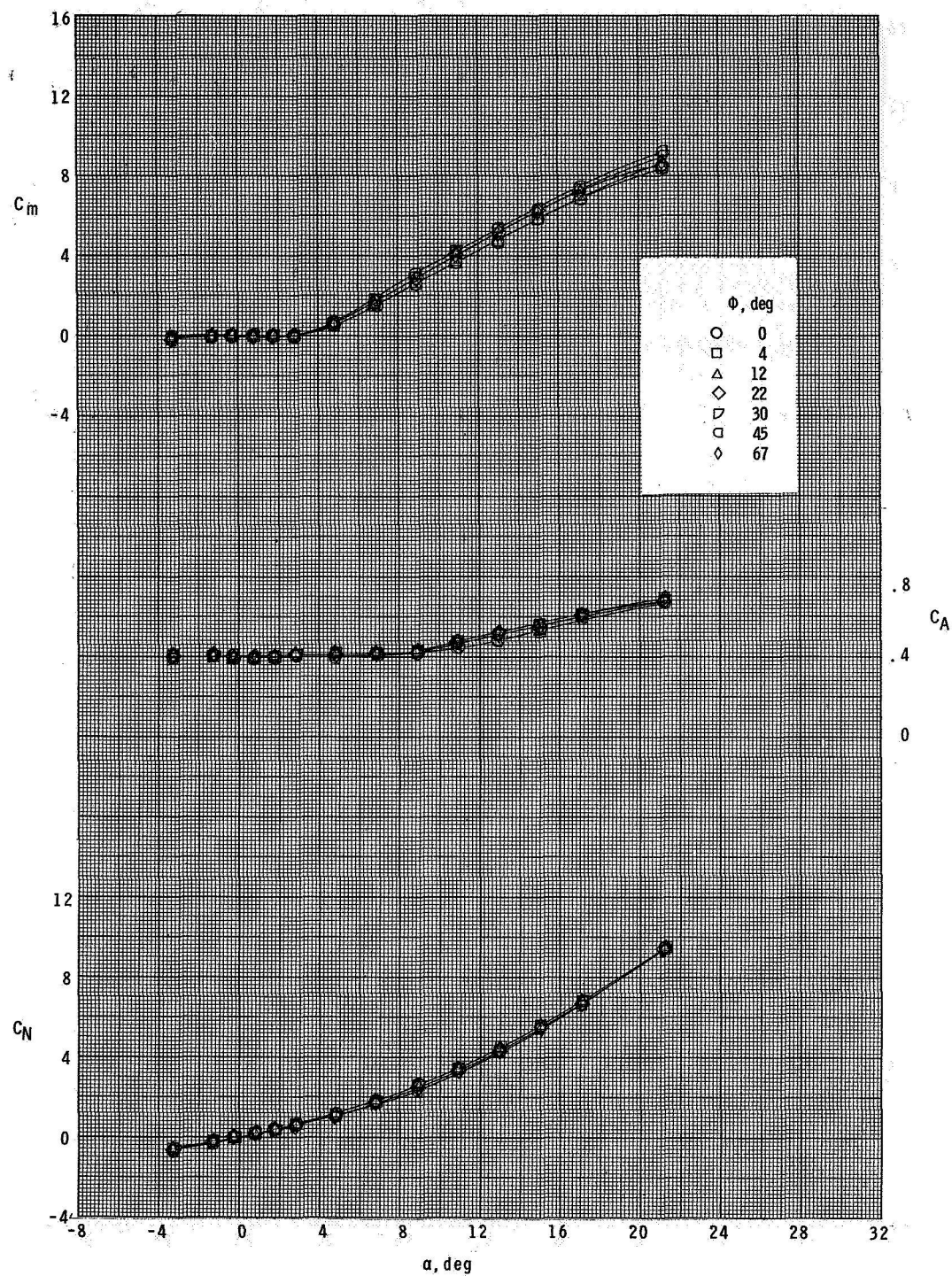
(b) Configuration $N_1E_2B_1F_2$.

Figure 8.- Continued.



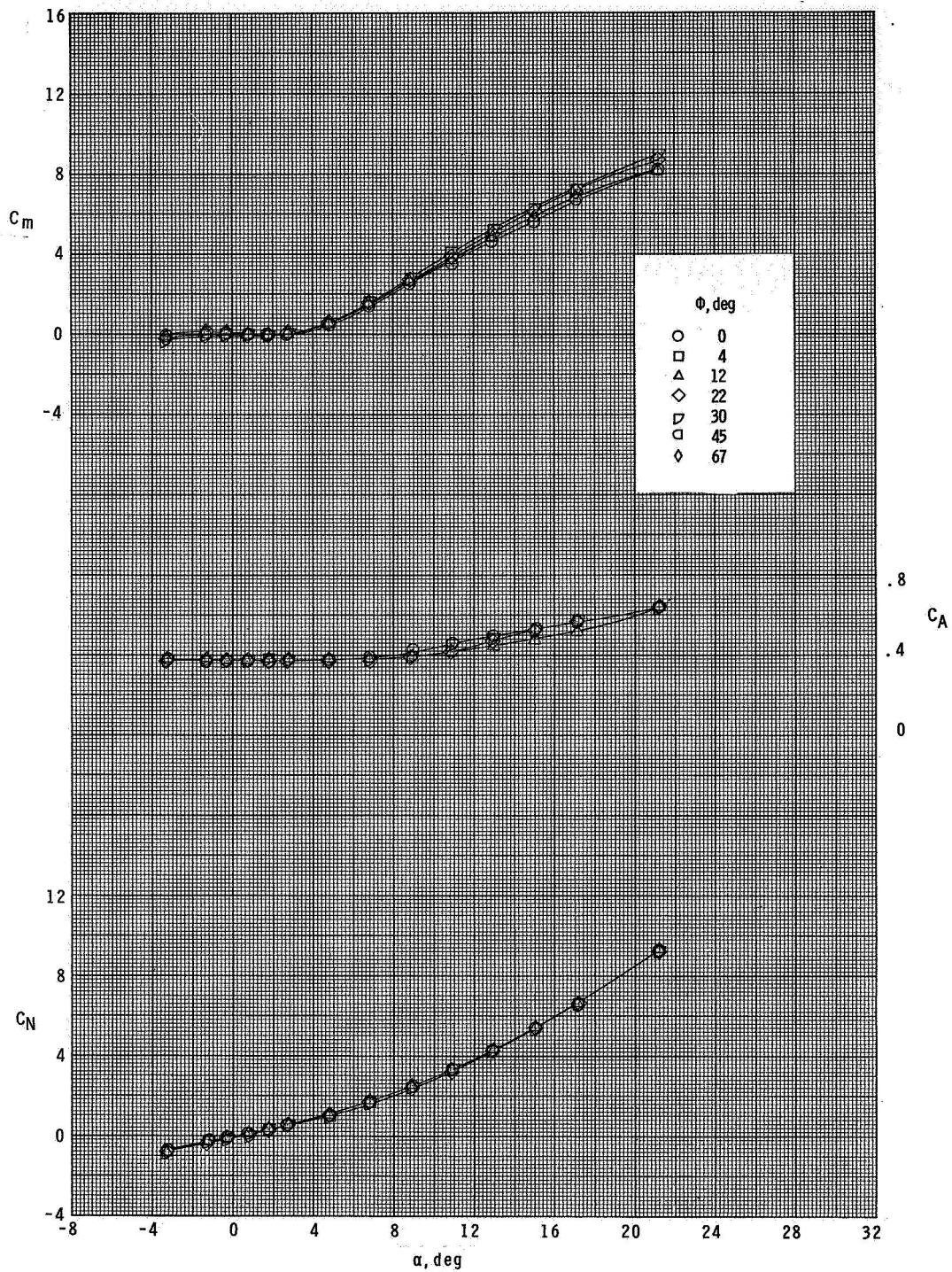
(c) Configuration $N_1E_2B_1F_5$.

Figure 8.- Concluded.



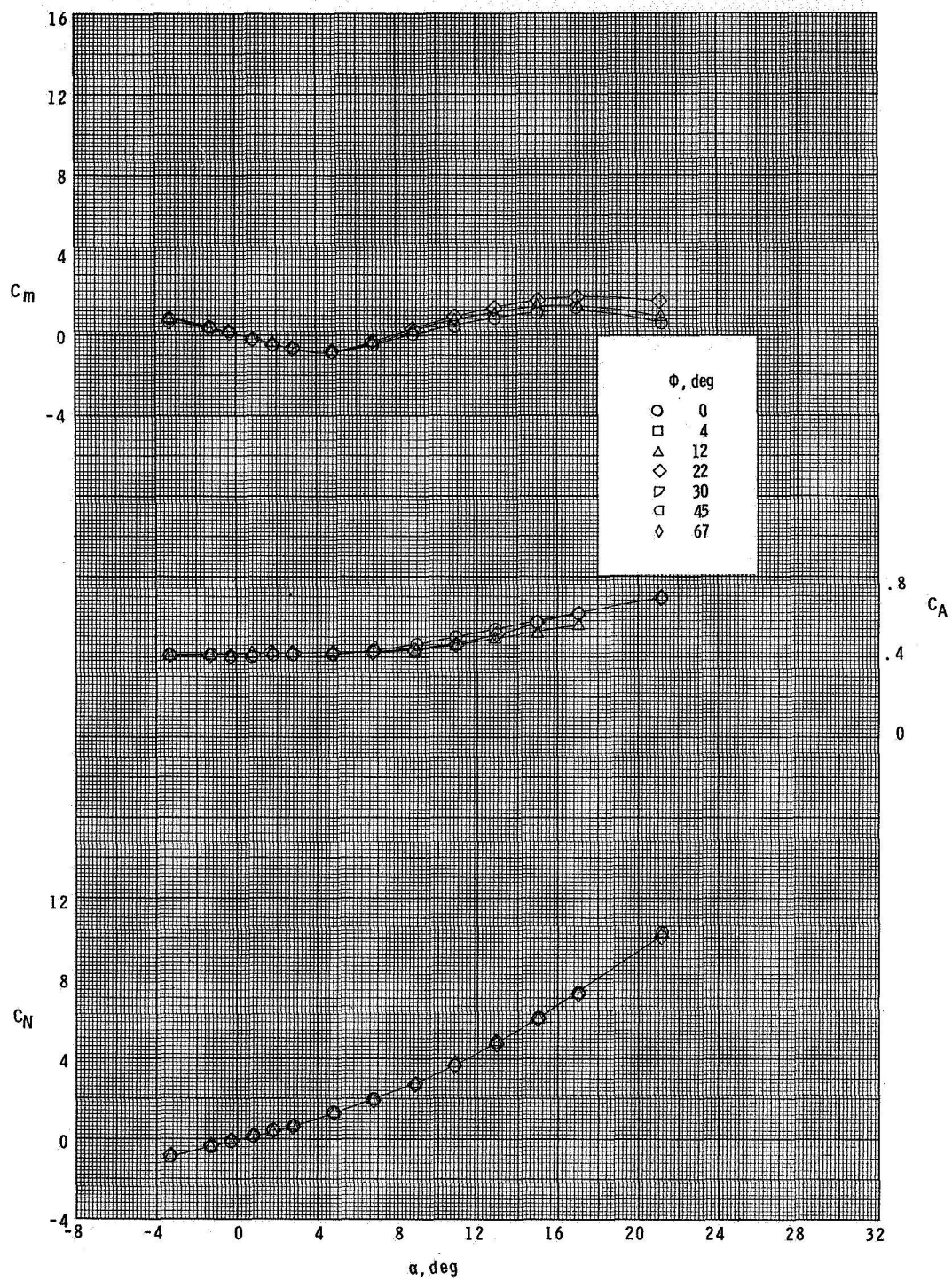
(a) Configuration $N_1E_2B_1F_1$.

Figure 9.- Effect of roll angle on longitudinal aerodynamic characteristics at $M = 4.63$.



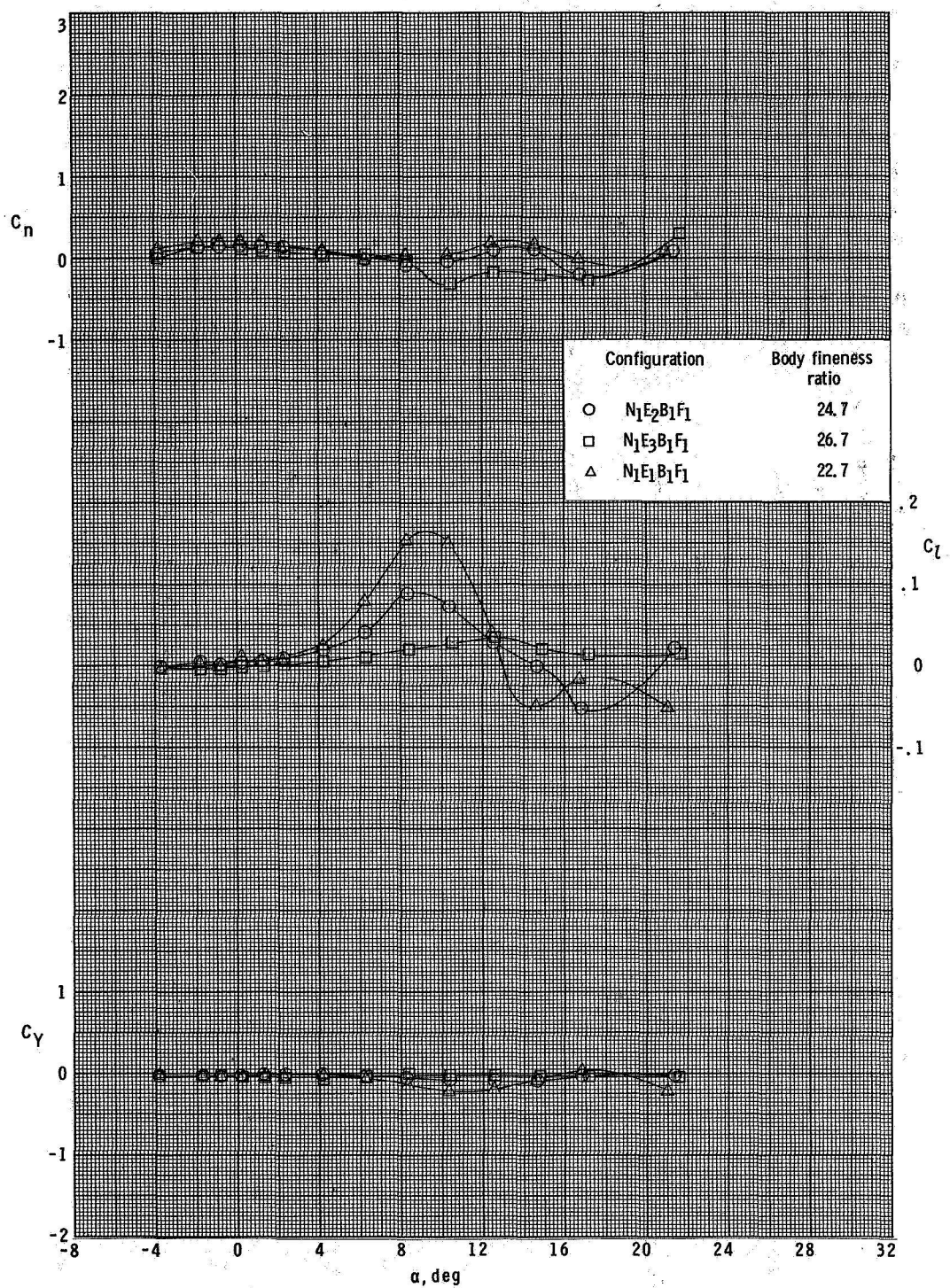
(b) Configuration $N_1E_2B_1F_2$.

Figure 9.- Continued.



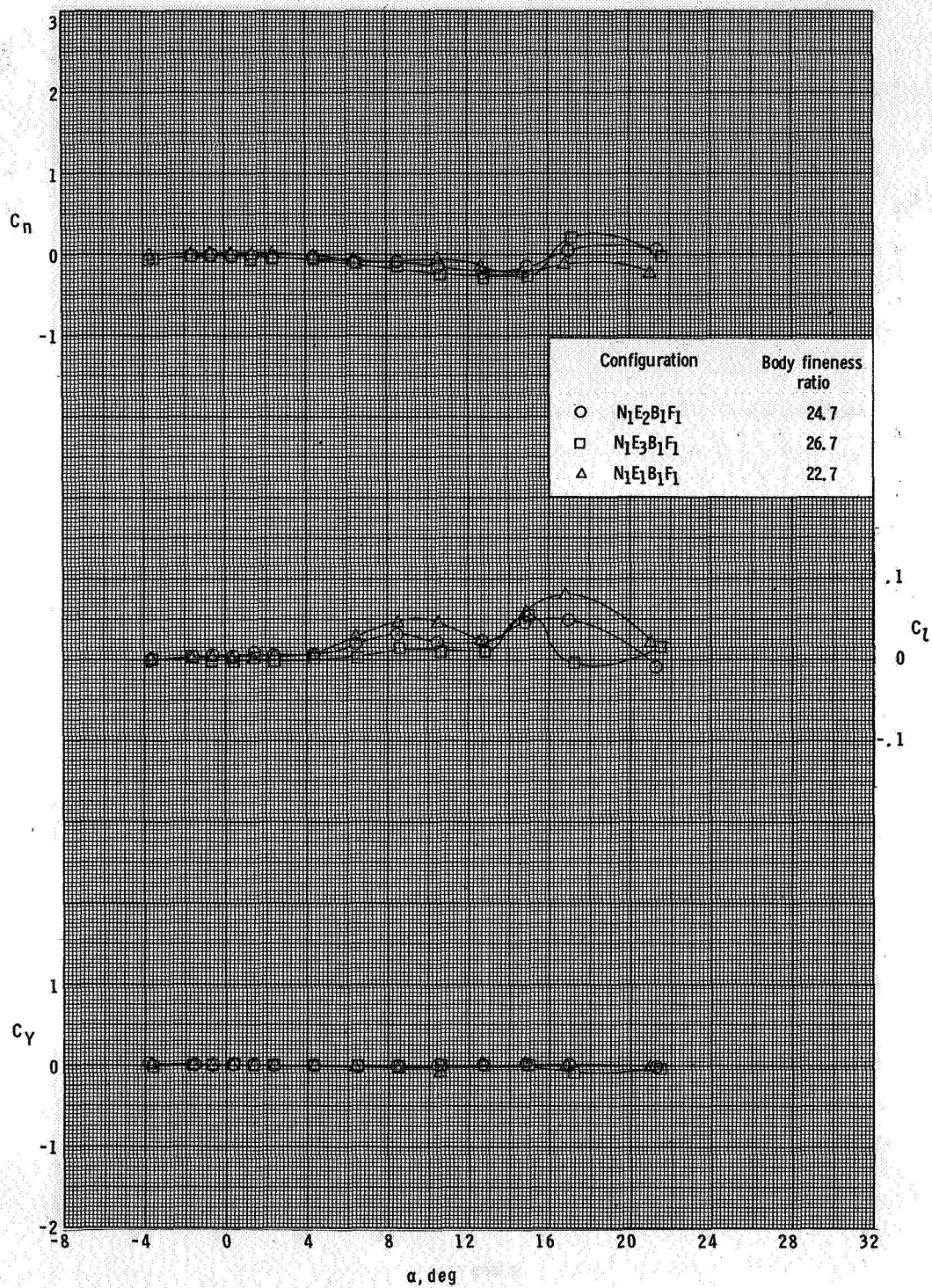
(c) Configuration $N_1E_2B_1F_5$.

Figure 9.- Concluded.



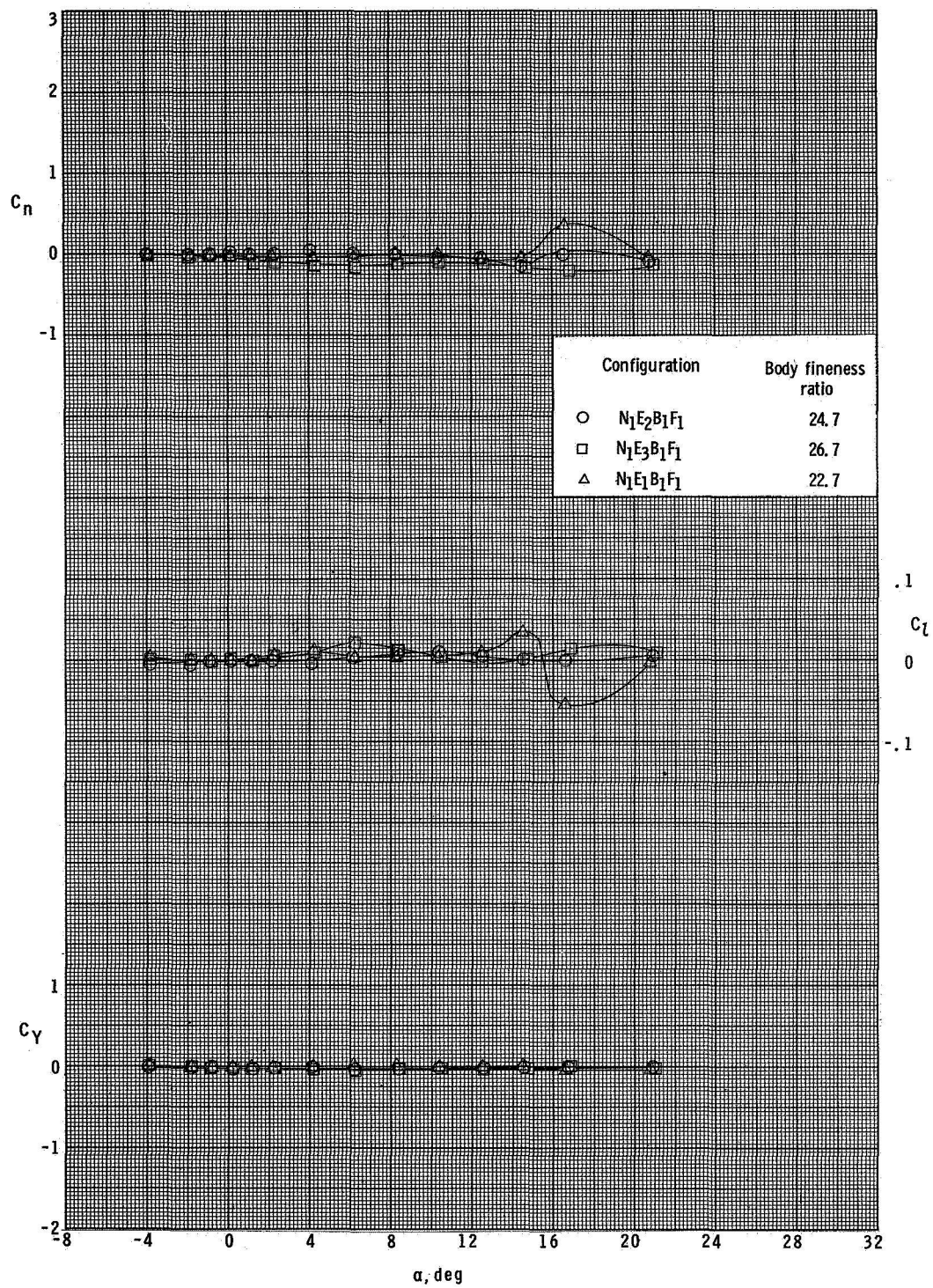
(a) $M = 2.30$.

Figure 10.- Effect of body fineness ratio on lateral aerodynamic characteristics. $\phi = 0^\circ$.



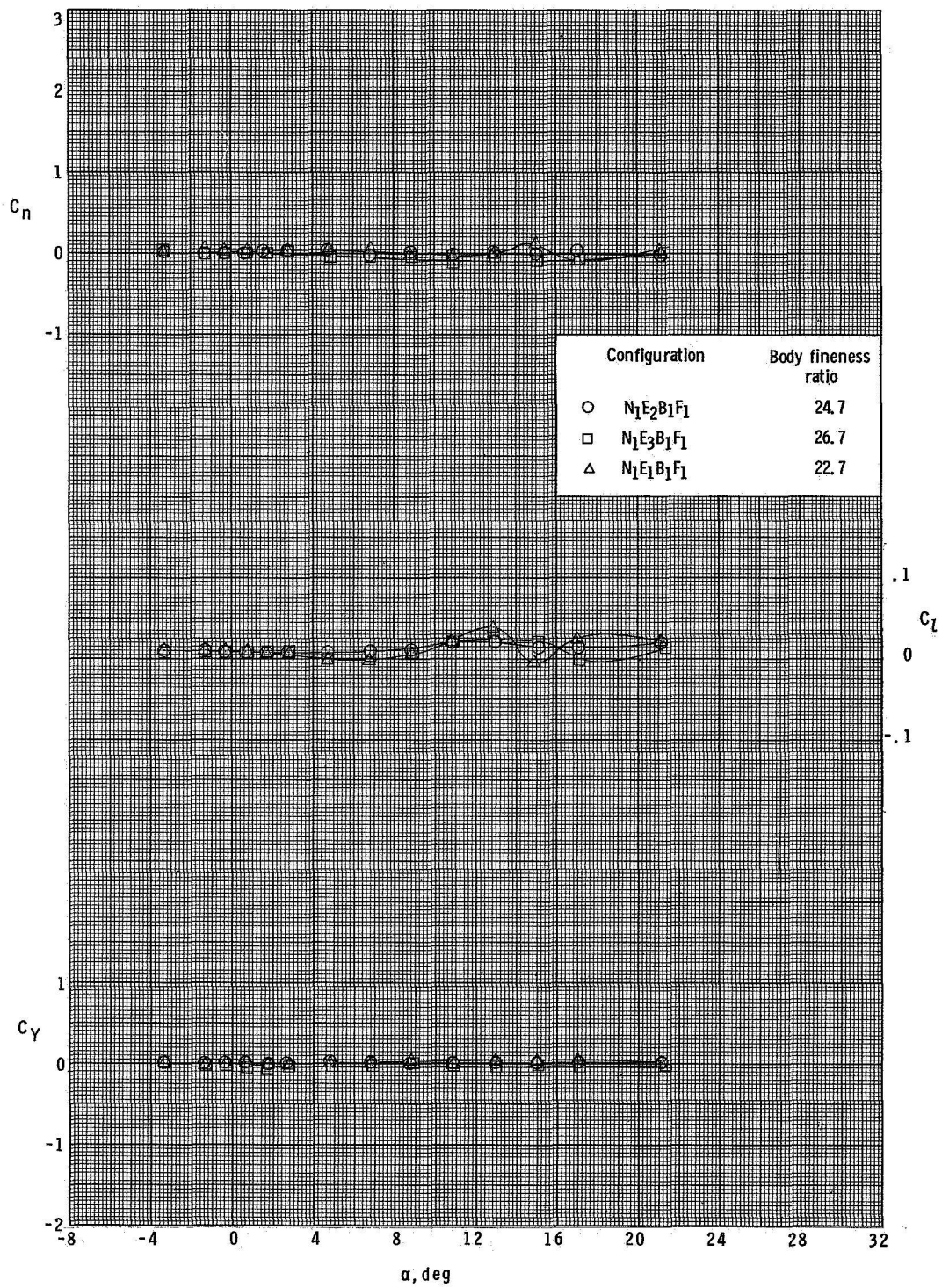
(b) $M = 2.96$.

Figure 10.- Continued.



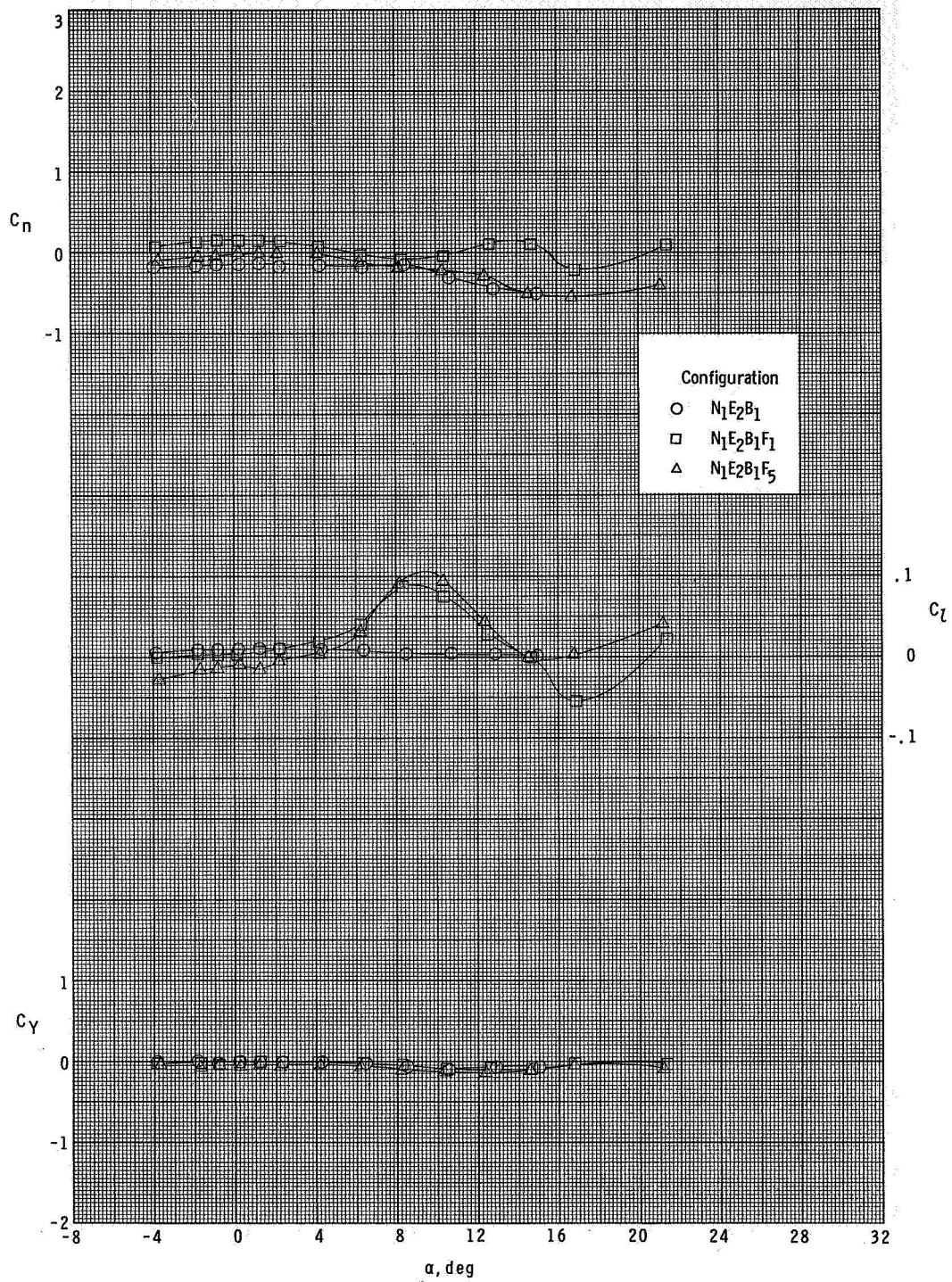
(c) $M = 3.95$.

Figure 10.- Continued.



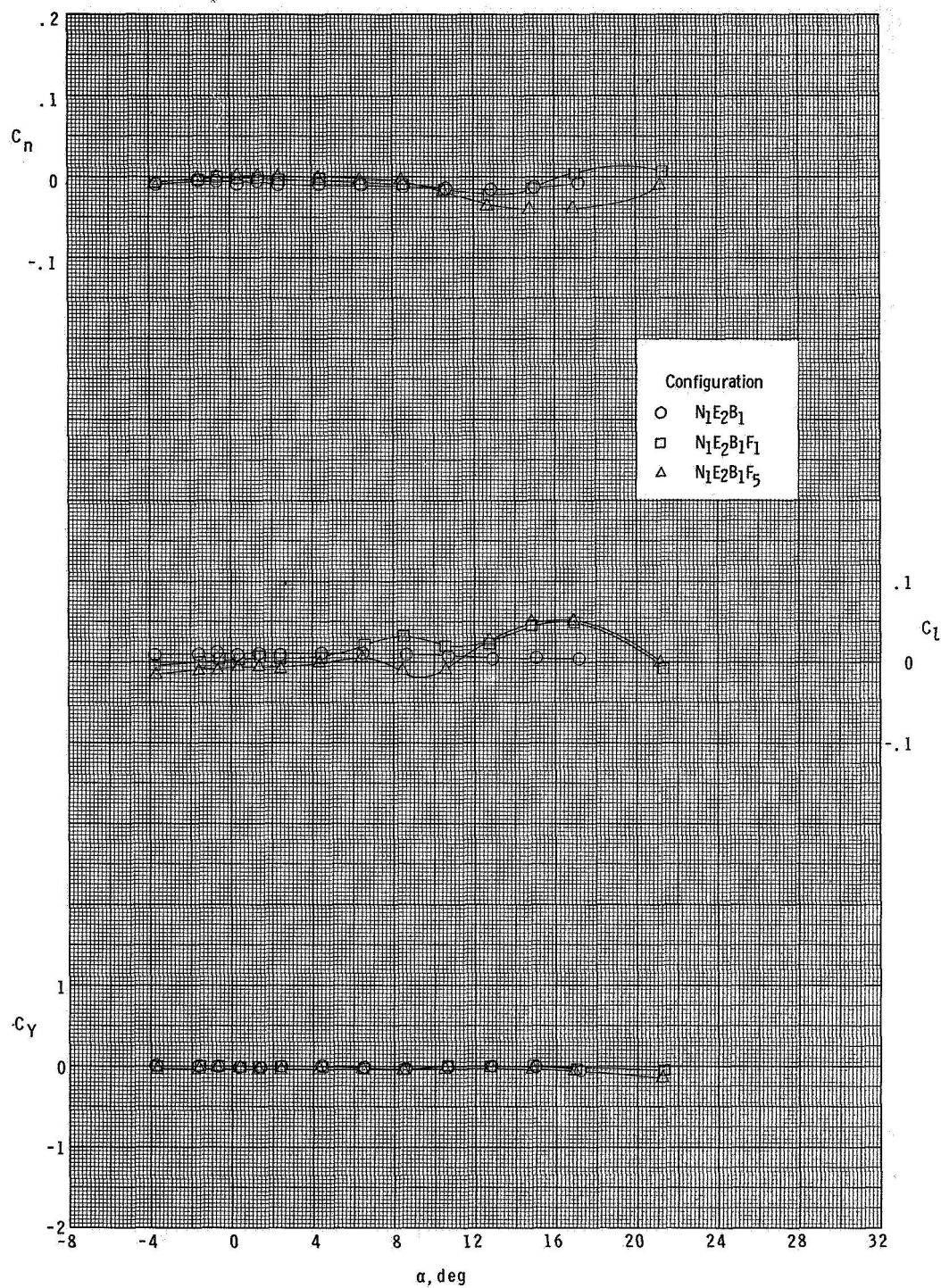
(d) $M = 4.63$.

Figure 10.- Concluded.



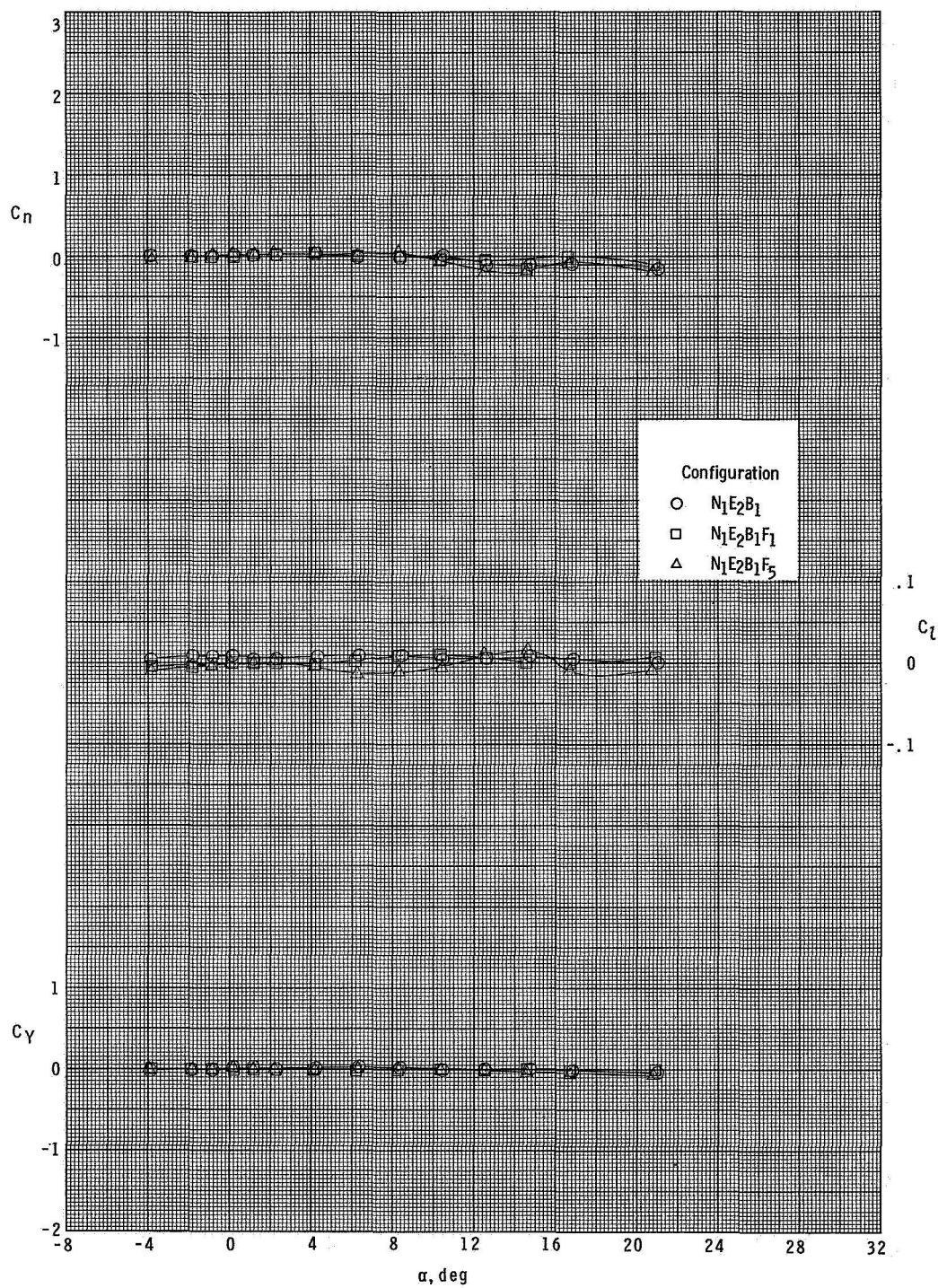
(a) $M = 2.30$.

Figure 11.- Effect of fins on lateral aerodynamic characteristics. $\phi = 0^\circ$.



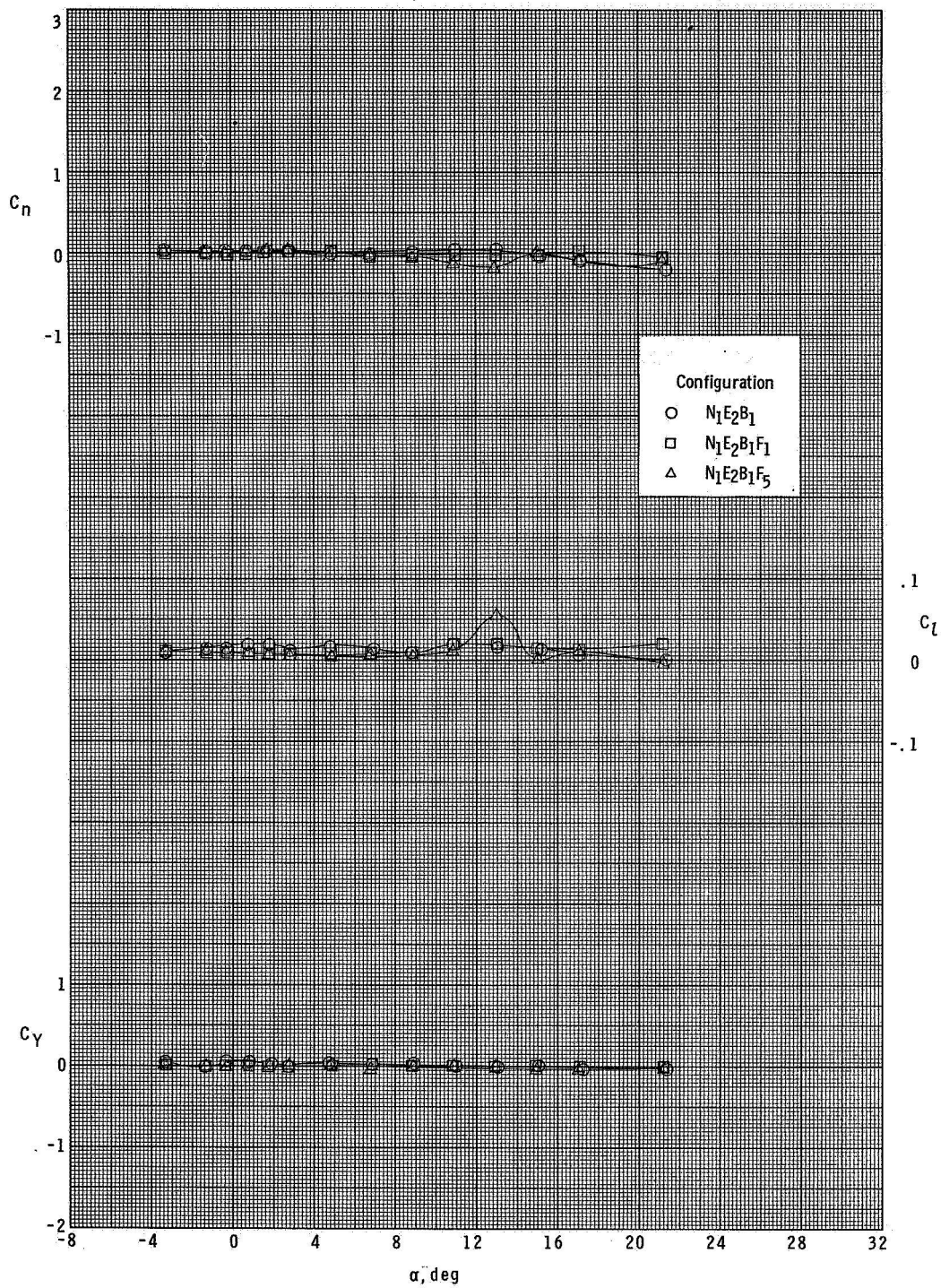
(b) $M = 2.96$.

Figure 11.- Continued.



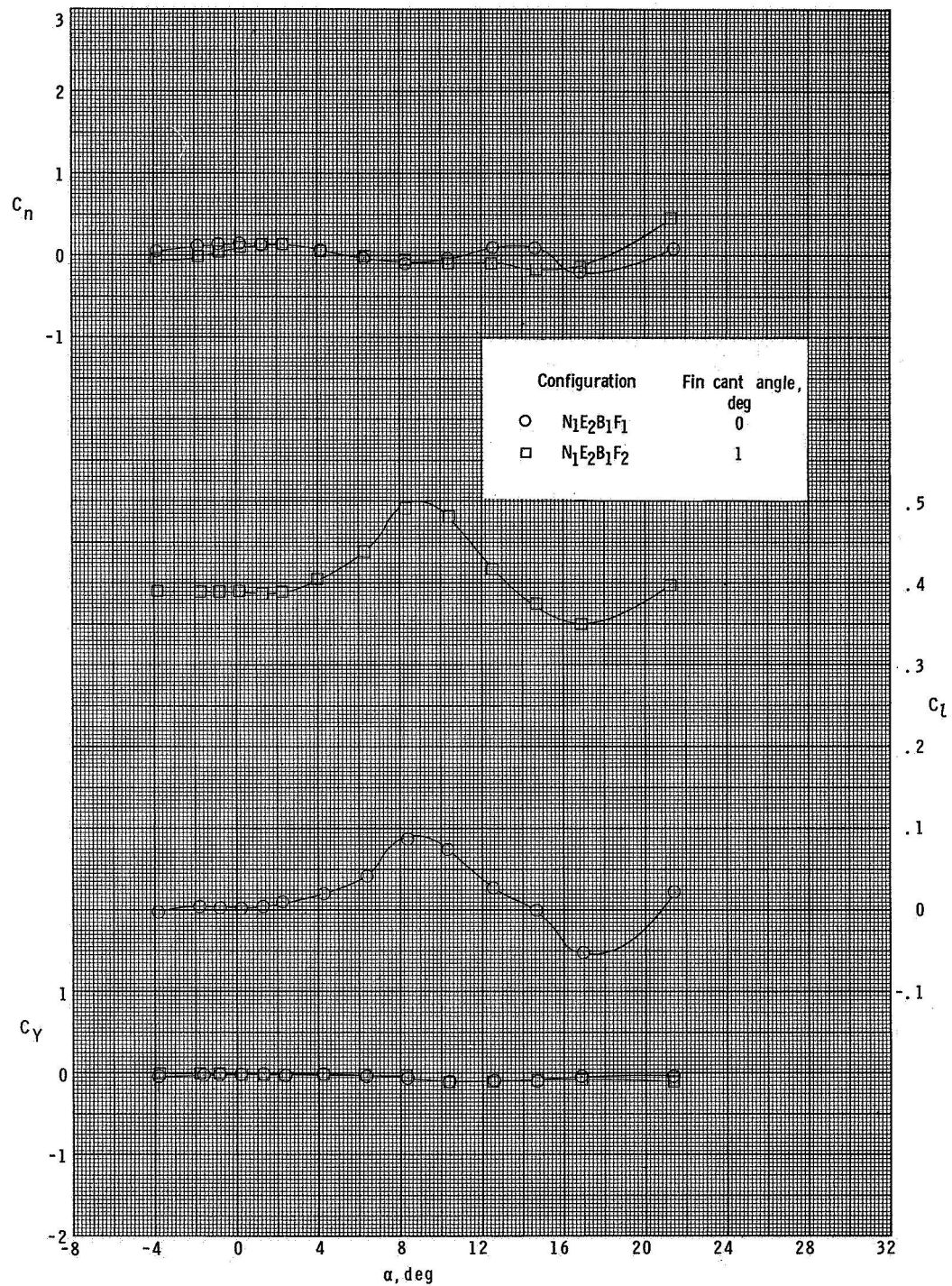
(c) $M = 3.95$.

Figure 11.- Continued.



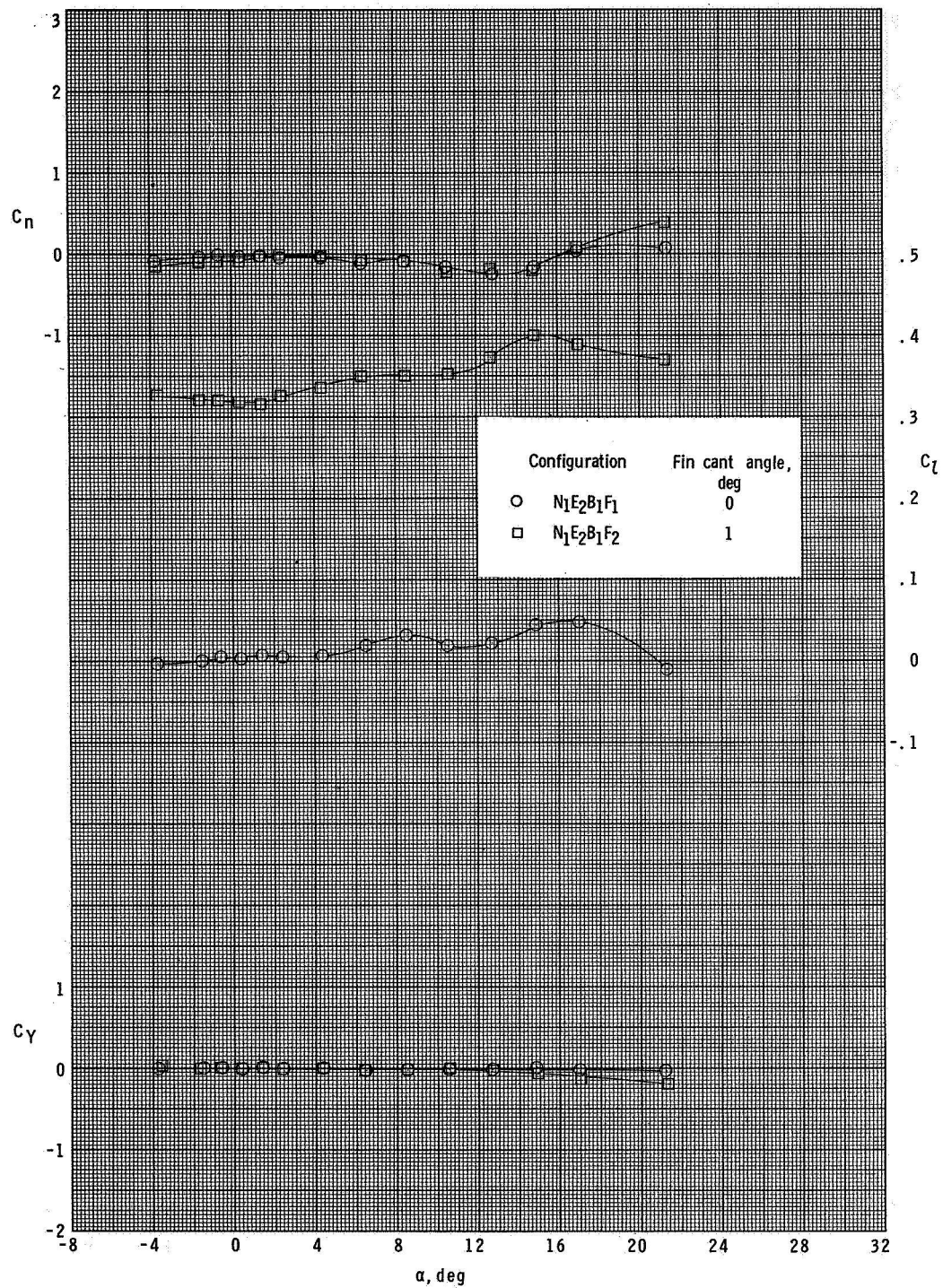
(d) $M = 4.63$.

Figure 11.- Concluded.



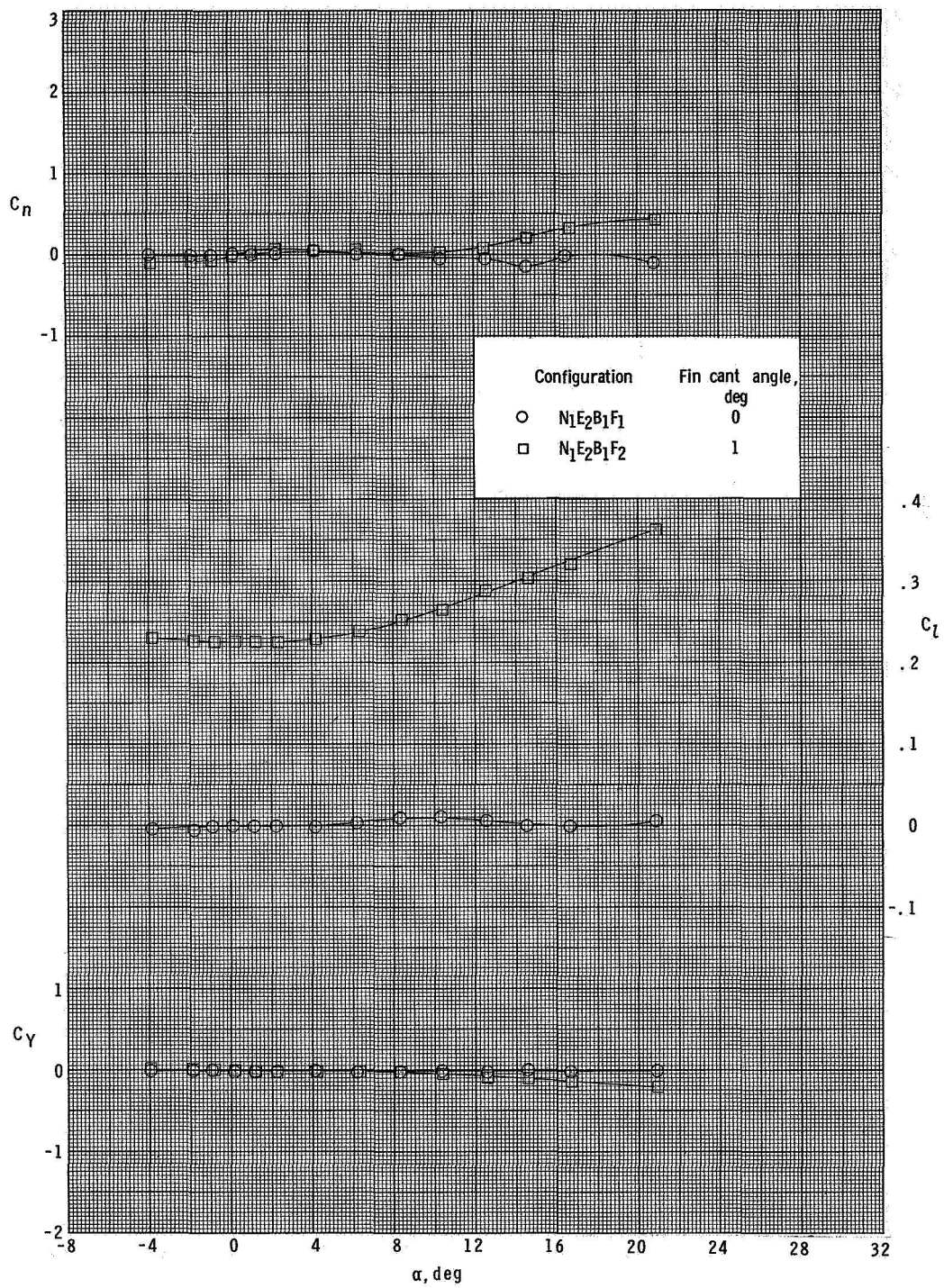
(a) $M = 2.30$.

Figure 12.- Effect of fin cant angle on lateral aerodynamic characteristics. $\phi = 0^\circ$.



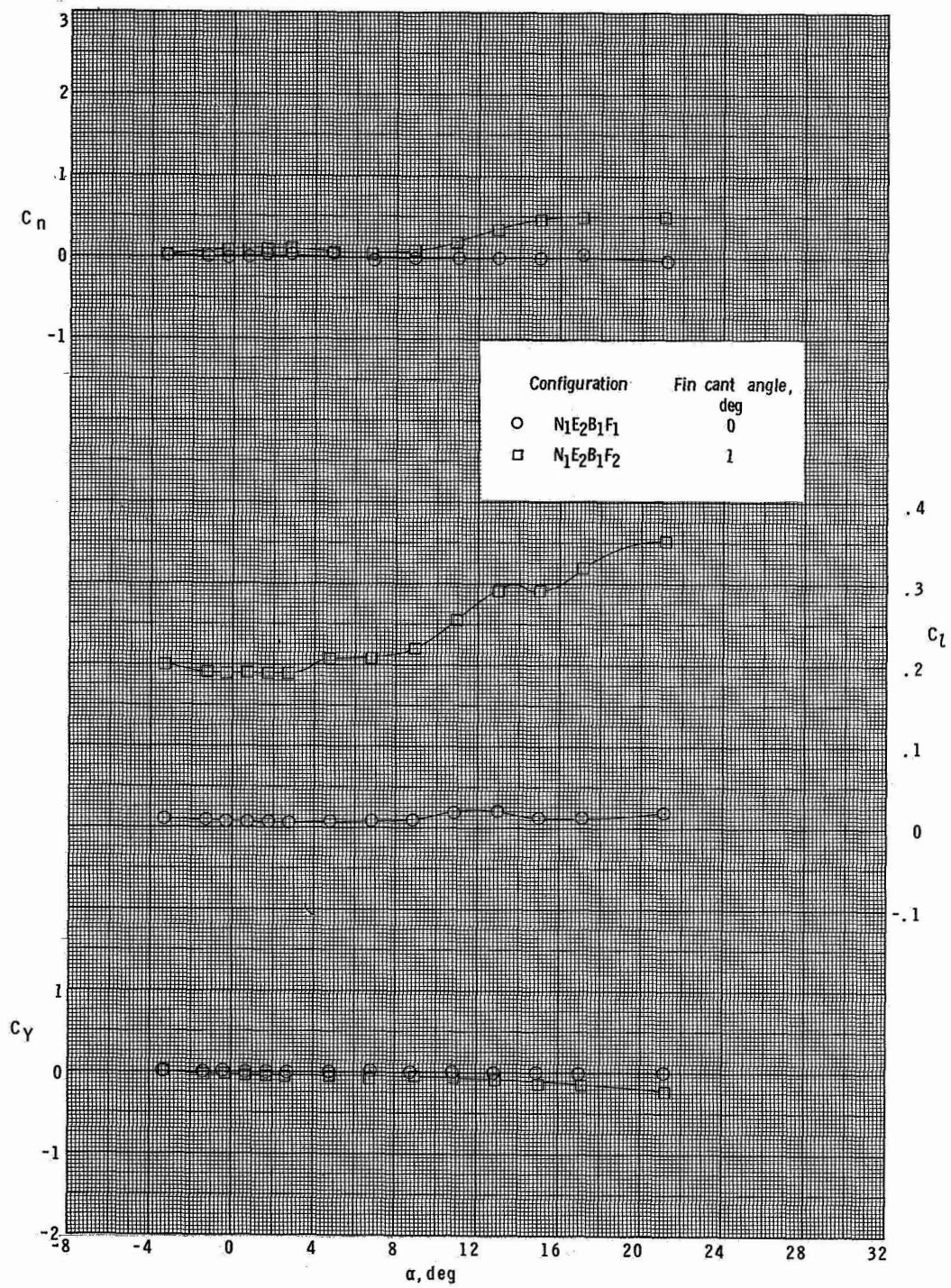
(b) $M = 2.96$.

Figure 12.- Continued.



(c) $M = 3.95$.

Figure 12.- Continued.



(d) $M = 4.63$.

Figure 12.- Concluded.

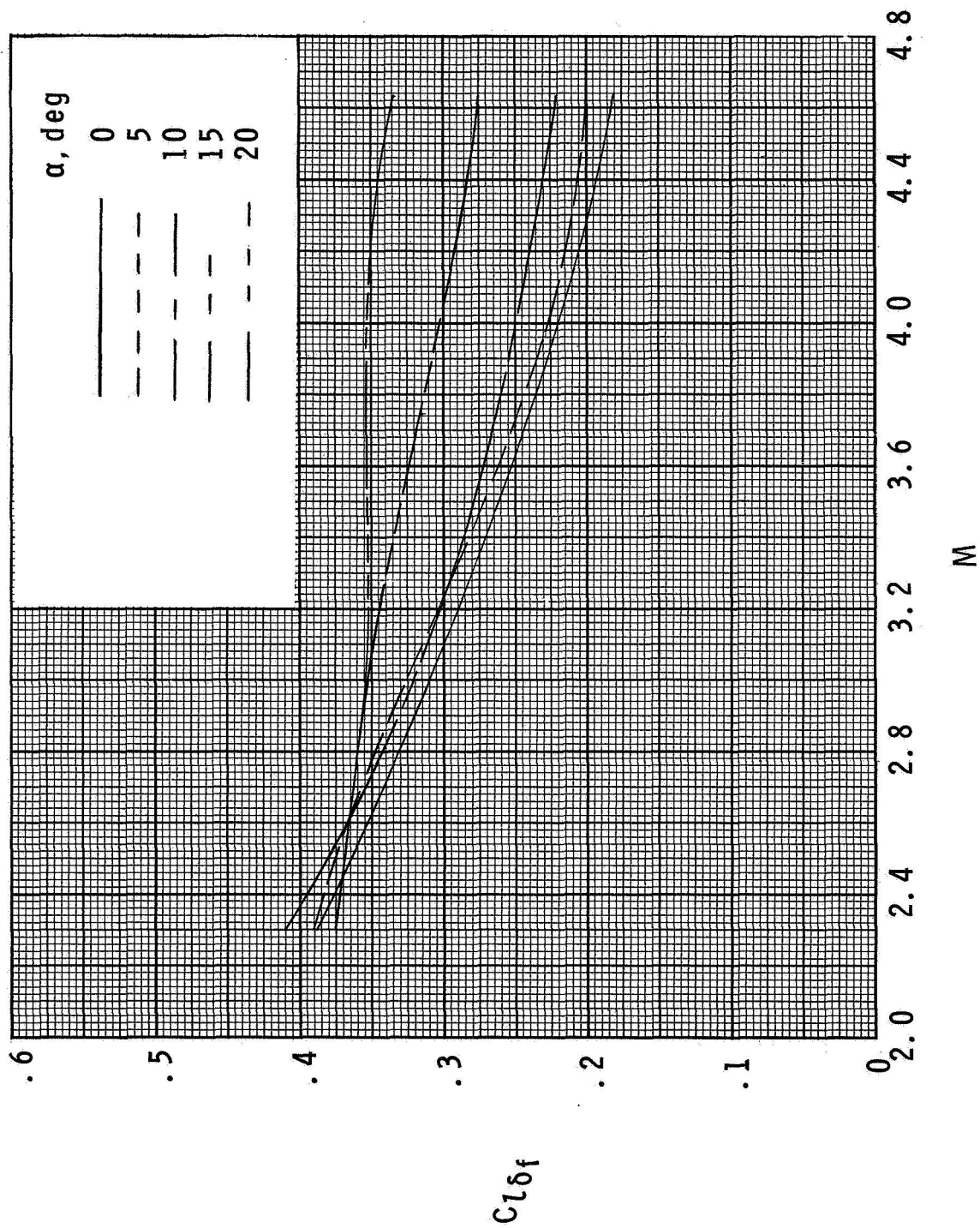
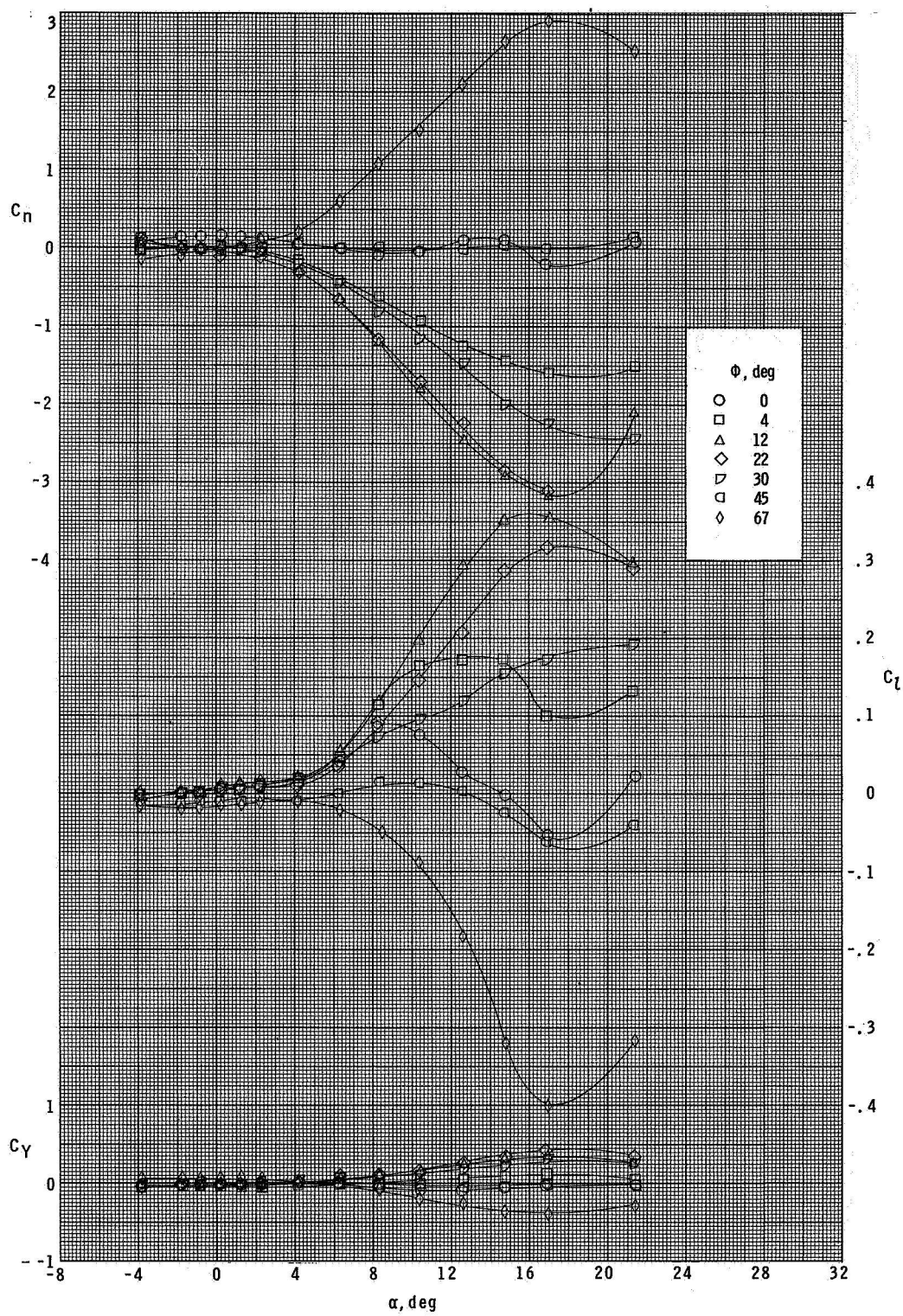
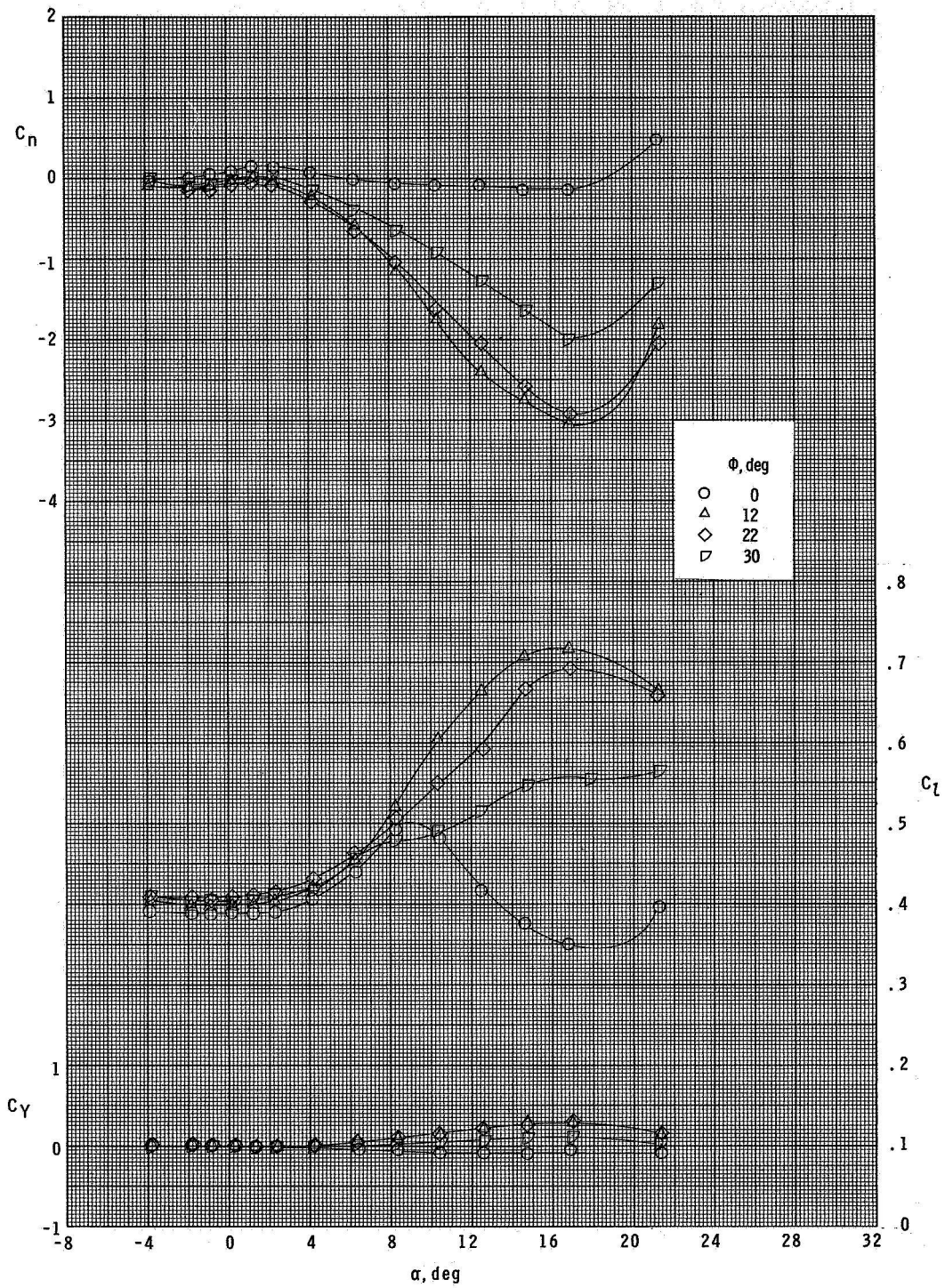


Figure 13.- Summary of effect of fin cant angle on rolling-moment coefficient. $\Delta \delta_f = 1^\circ$.



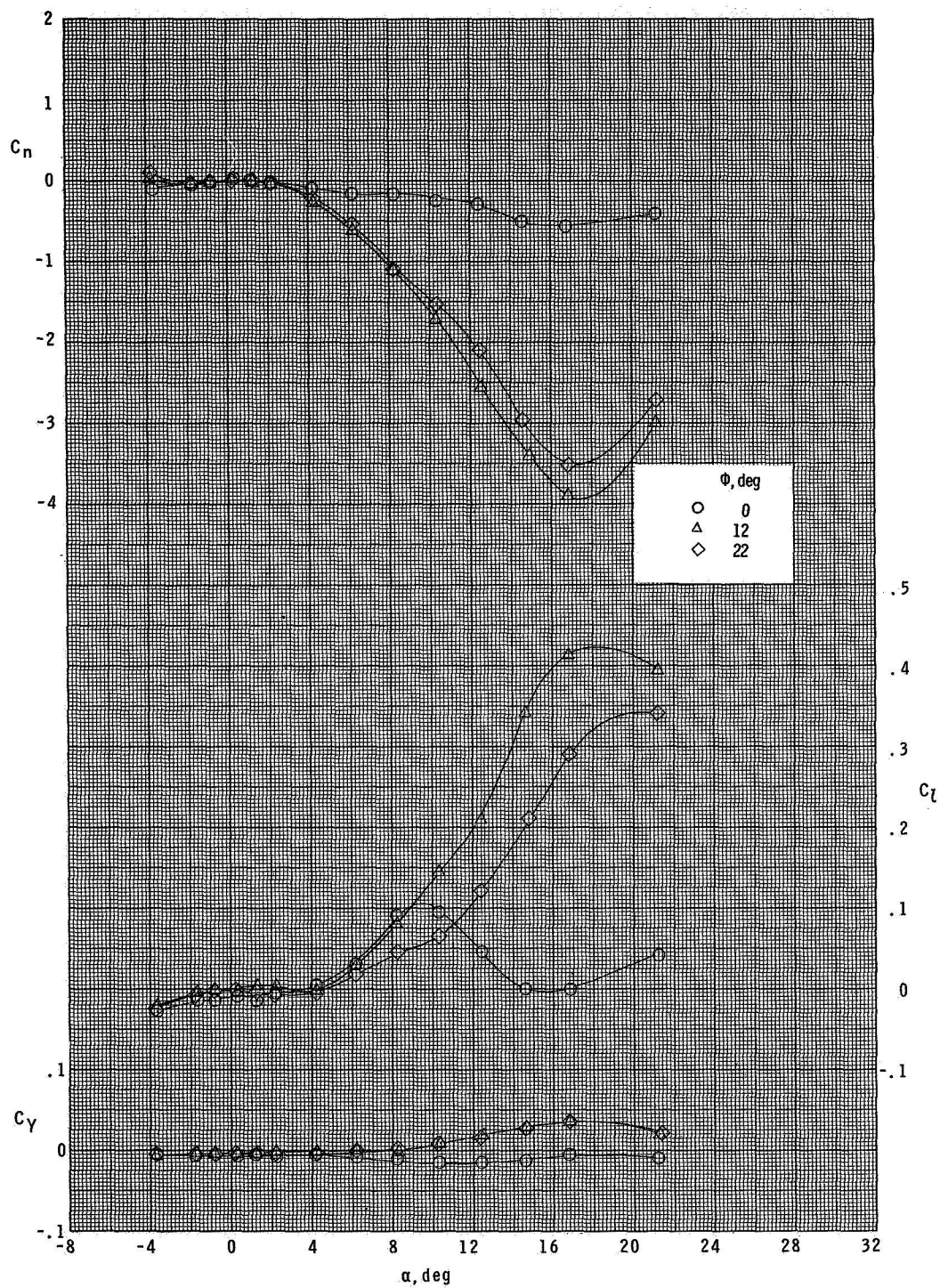
(a) Configuration $N_1E_2B_1F_1$.

Figure 14.- Effect of roll angle on lateral aerodynamic characteristics at $M = 2.30$.



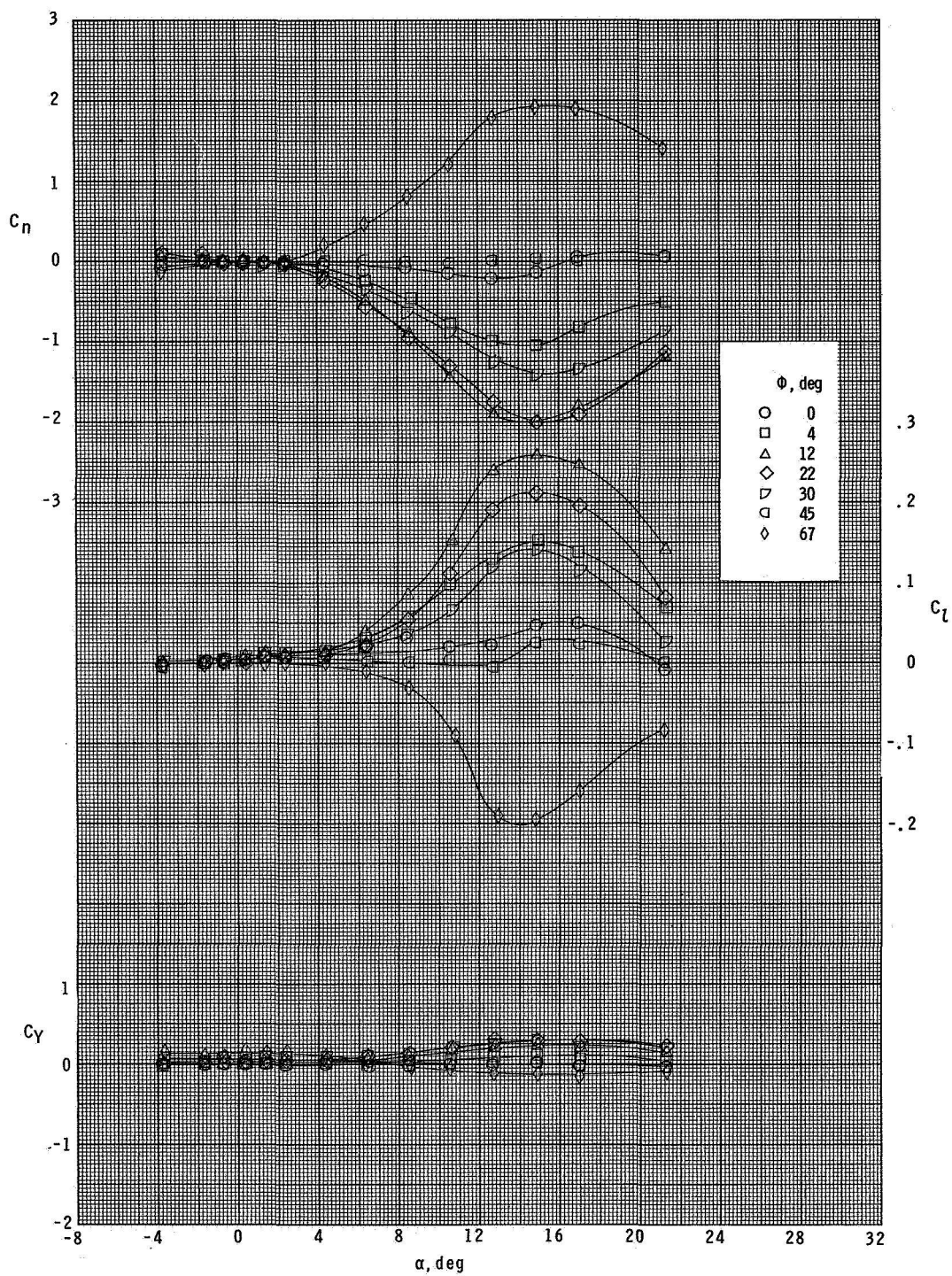
(b) Configuration $N_1E_2B_1F_2$.

Figure 14.- Continued.



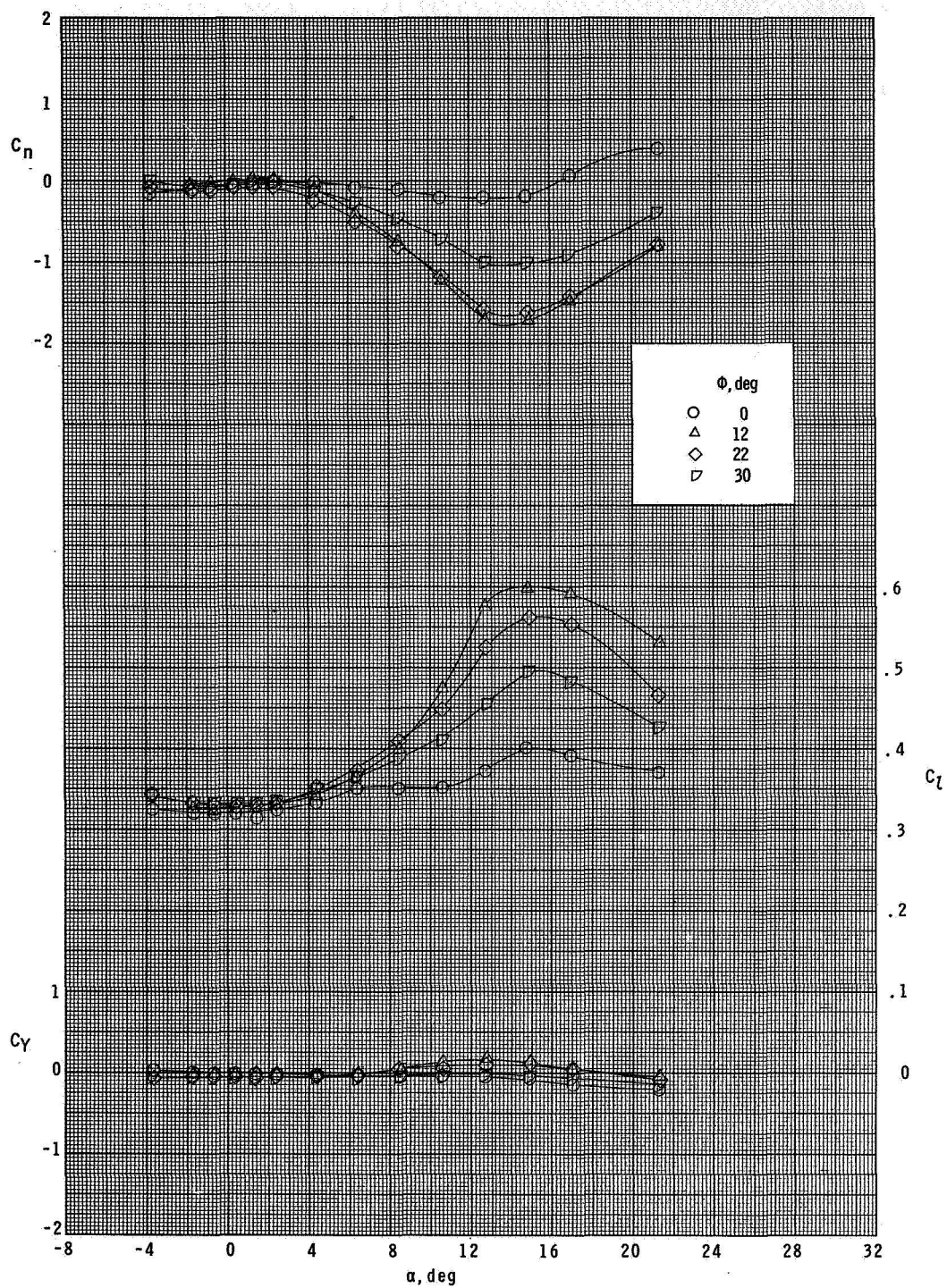
(c) Configuration $N_1E_2B_1F_5$.

Figure 14.- Concluded.



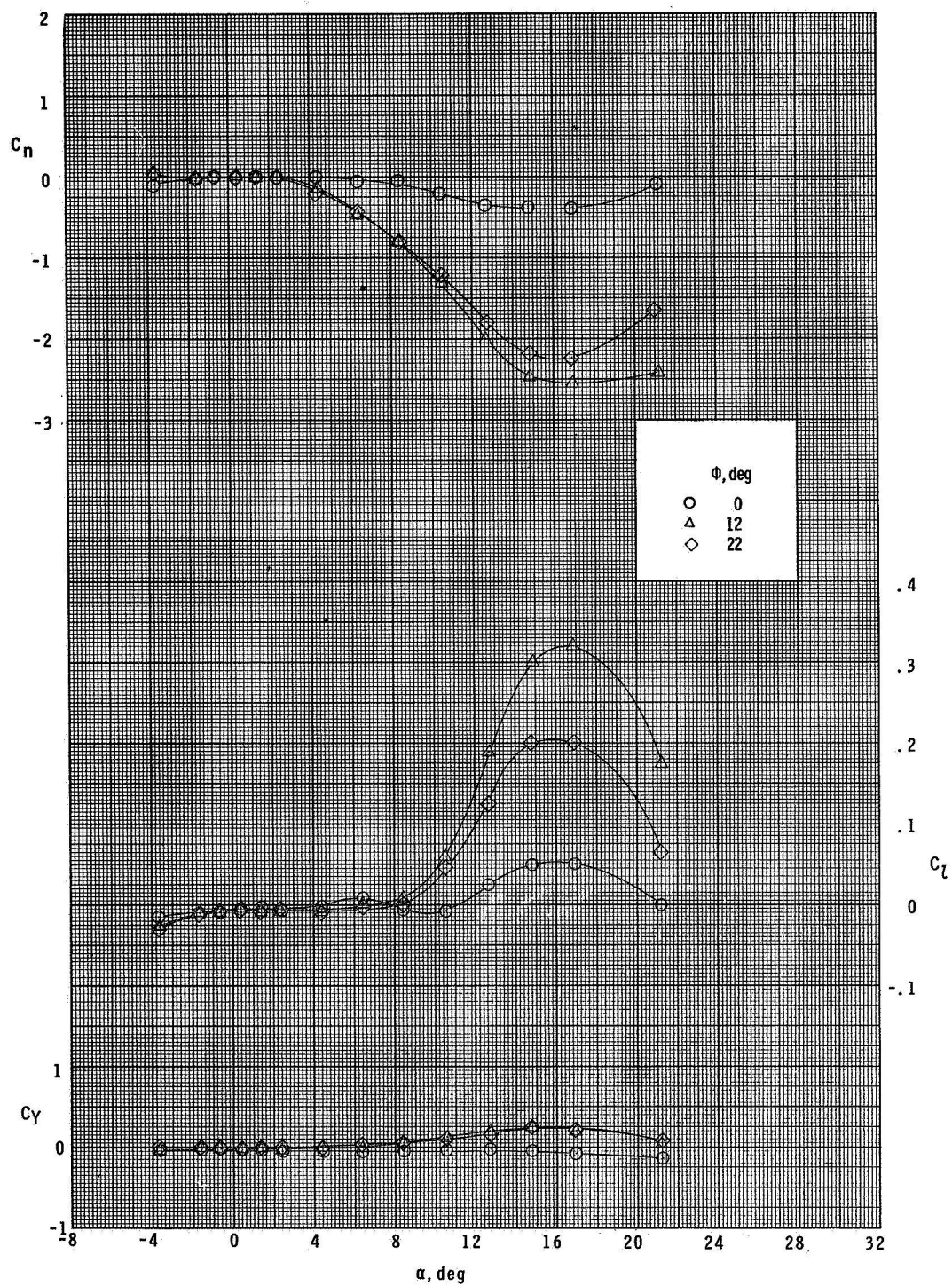
(a) Configuration $N_1E_2B_1F_1$.

Figure 15.- Effect of roll angle on lateral aerodynamic characteristics at $M = 2.96$.



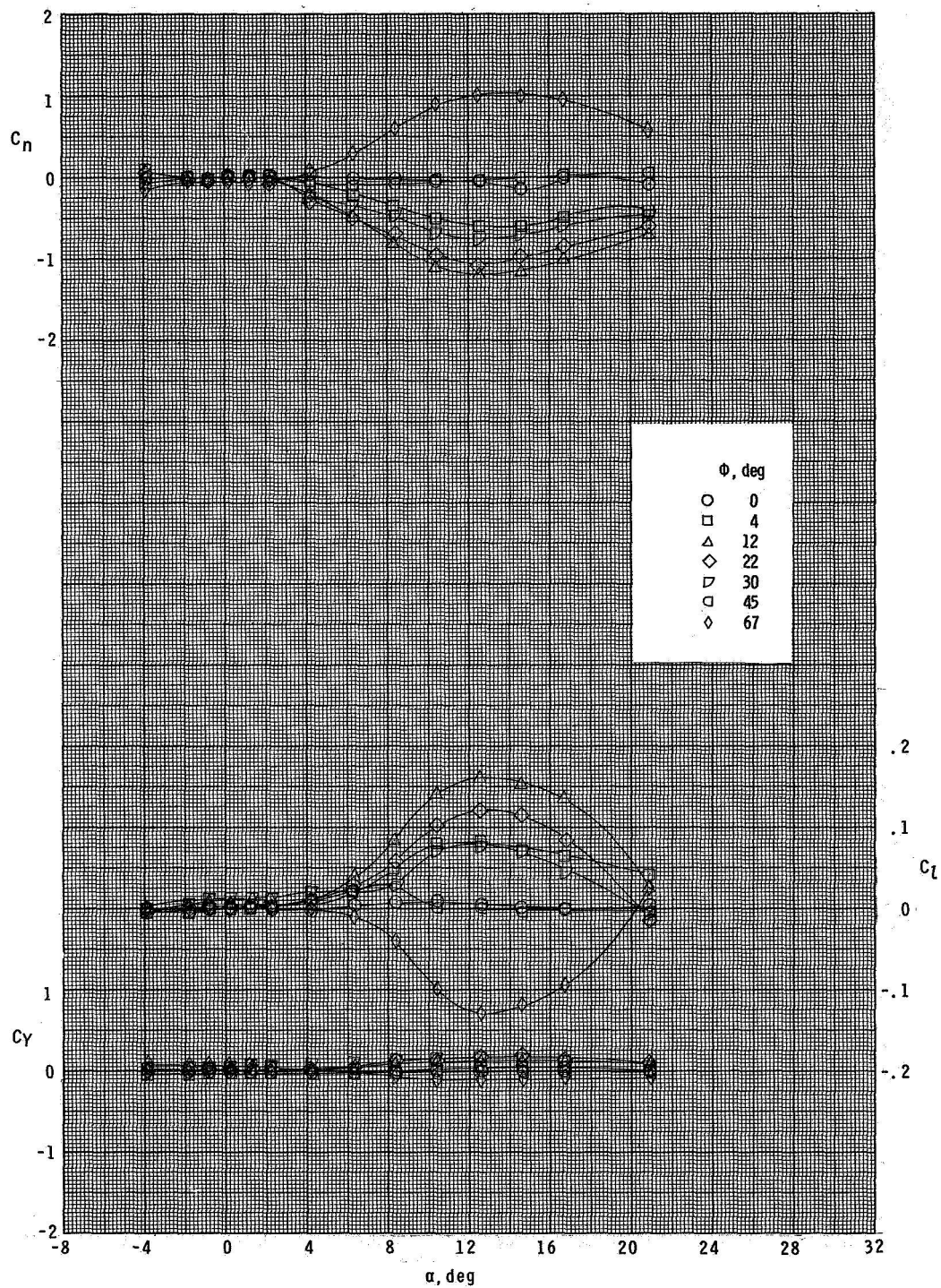
(b) Configuration $N_1E_2B_1F_2$.

Figure 15.- Continued.



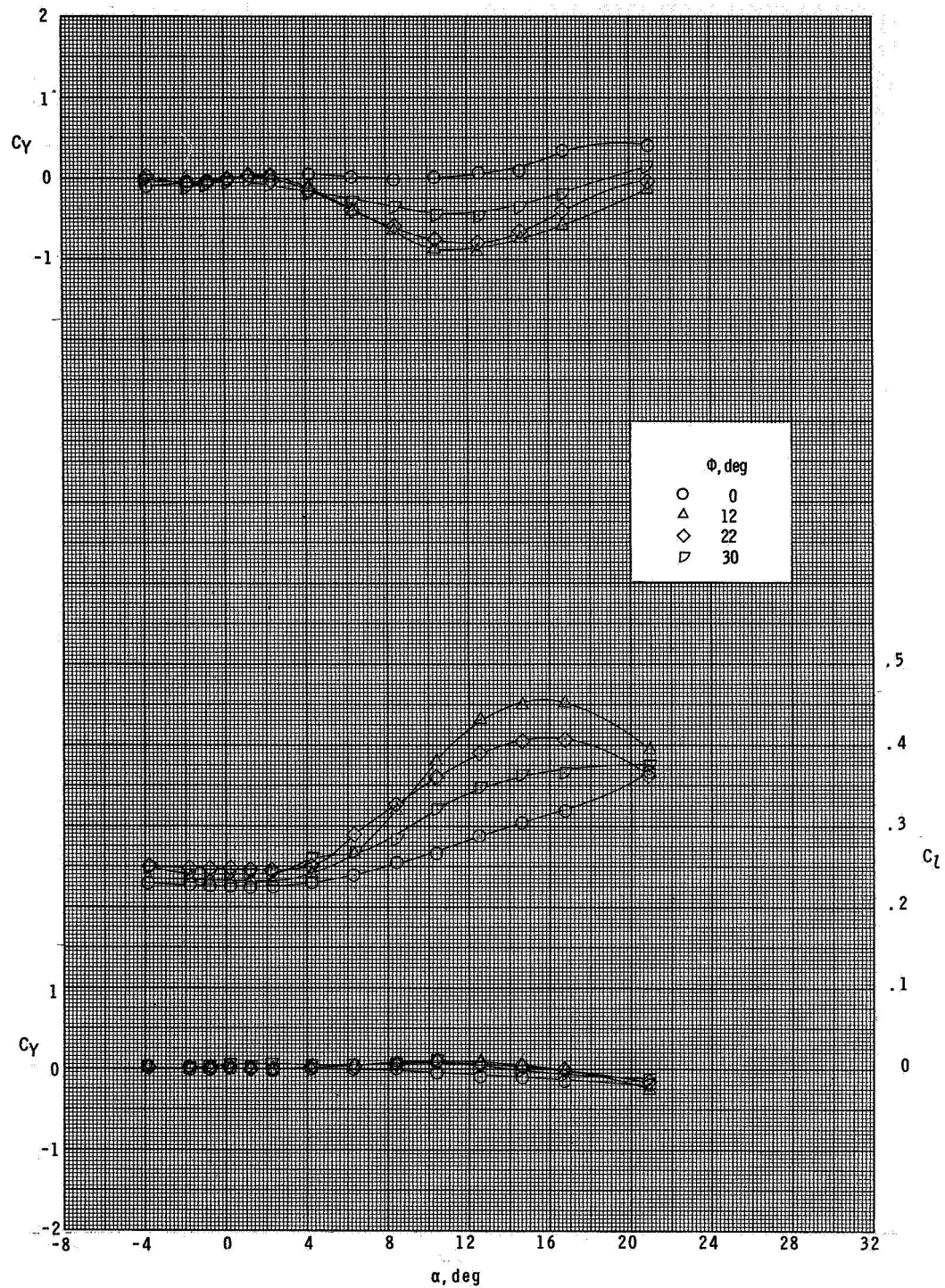
(c) Configuration $N_1E_2B_1F_5$.

Figure 15.- Concluded.



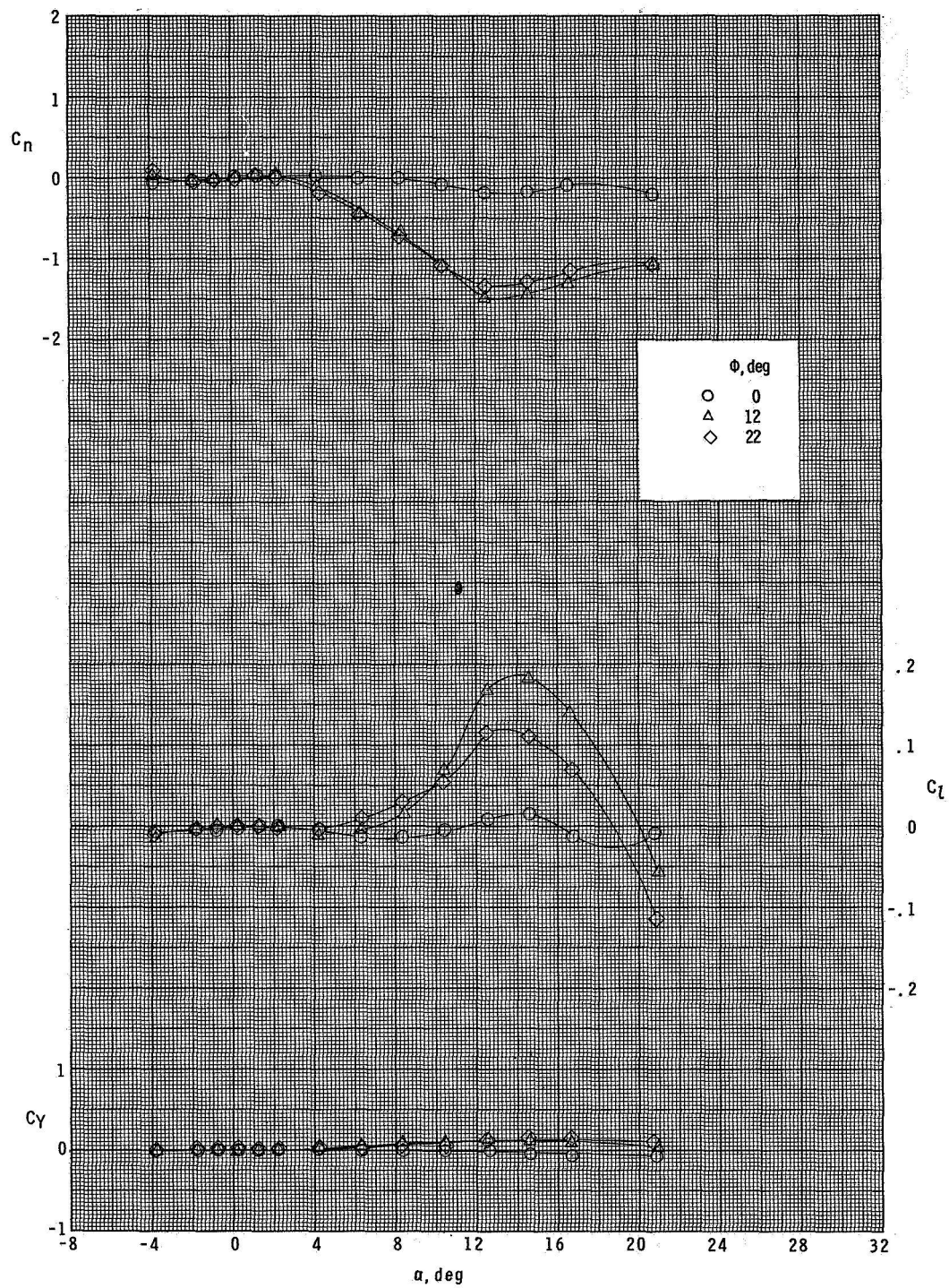
(a) Configuration $N_1E_2B_1F_1$.

Figure 16.- Effect of roll angle on lateral aerodynamic characteristics at $M^* = 3.95$.



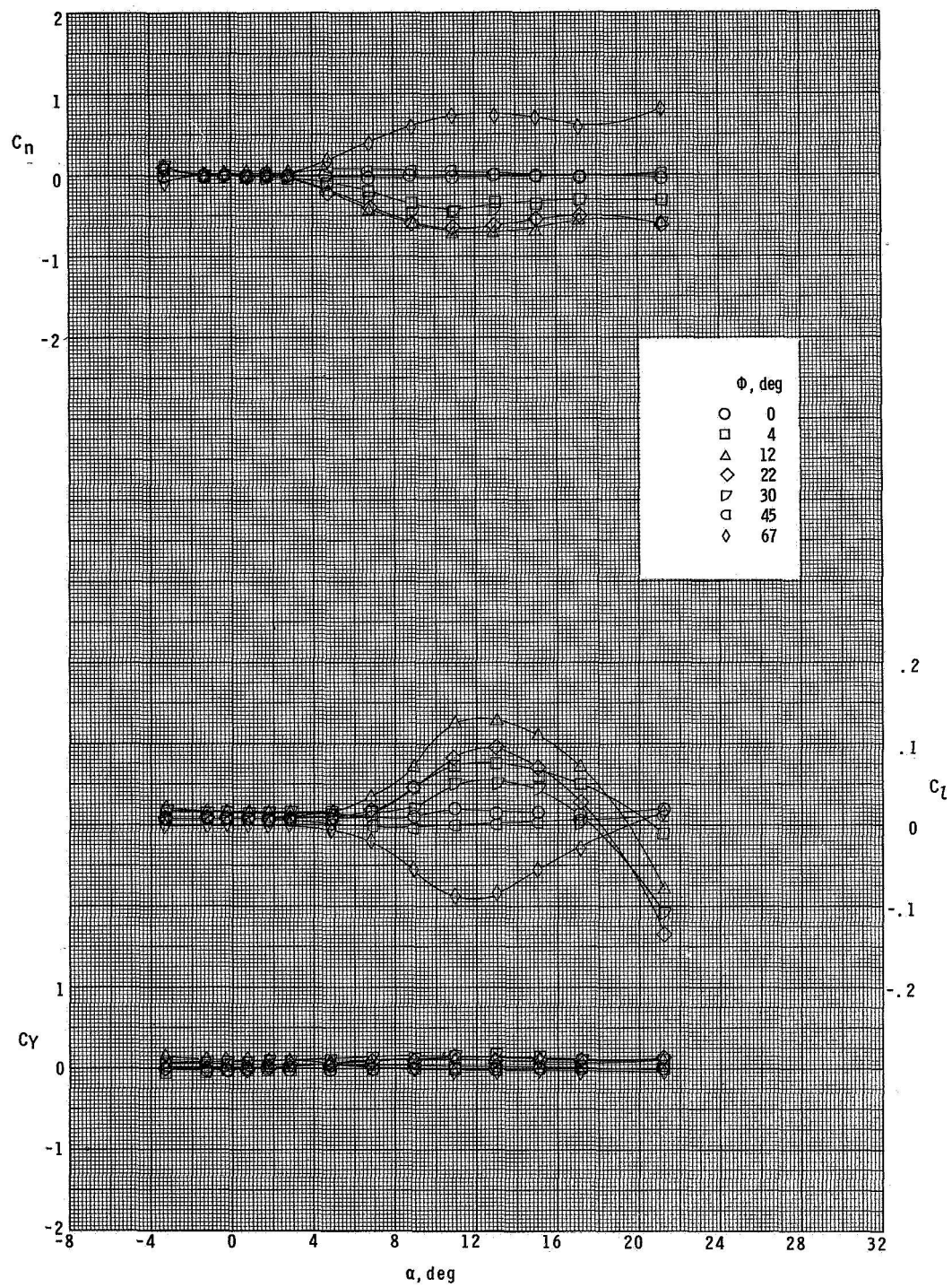
(b) Configuration $N_1E_2B_1F_2$.

Figure 16.- Continued.



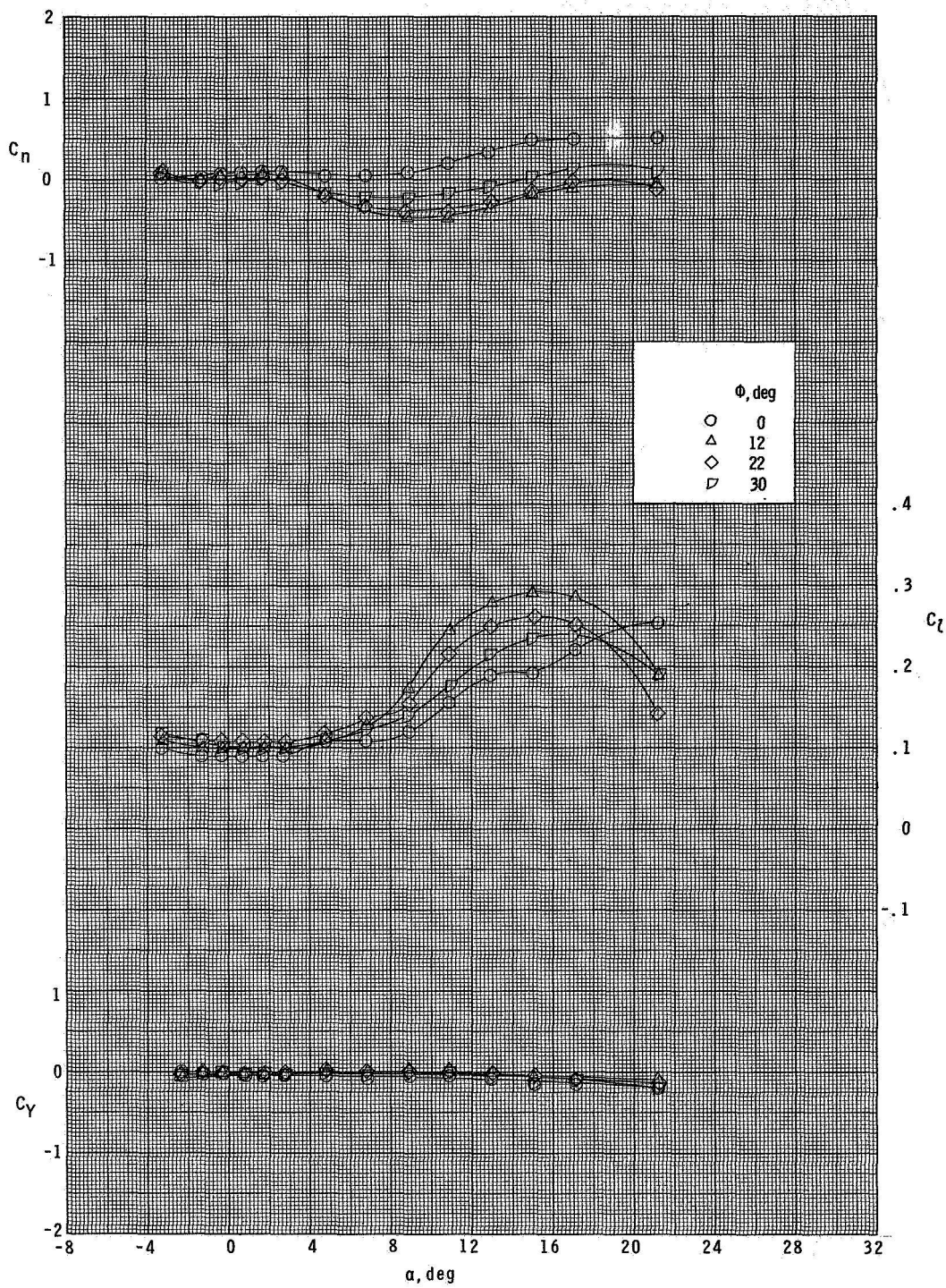
(c) Configuration $N_1E_2B_1F_5$.

Figure 16.- Concluded.



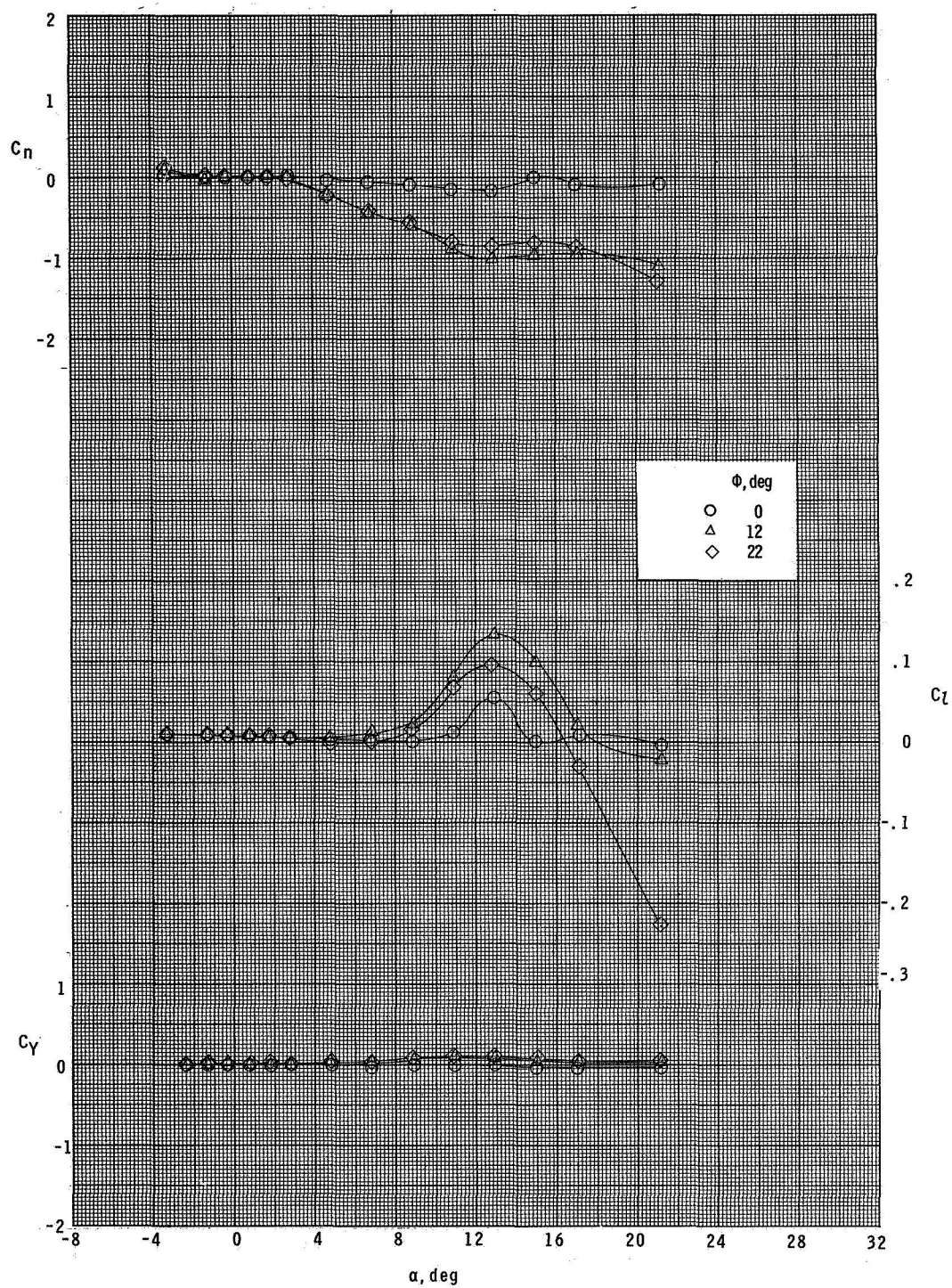
(a) Configuration $N_1E_2B_1F_1$.

Figure 17.- Effect of roll angle on lateral aerodynamic characteristics at $M = 4.63$.



(b) Configuration $N_1E_2B_1F_2$.

Figure 17.- Continued.



(c) Configuration $N_1E_2B_1F_5$.

Figure 17.- Concluded.

POSTMASTER: If Undeliverable (Section 158
Postal Manual) Do Not Return

"The aeronautical and space activities of the United States shall be conducted so as to contribute . . . to the expansion of human knowledge of phenomena in the atmosphere and space. The Administration shall provide for the widest practicable and appropriate dissemination of information concerning its activities and the results thereof."

— NATIONAL AERONAUTICS AND SPACE ACT OF 1958

NASA SCIENTIFIC AND TECHNICAL PUBLICATIONS

TECHNICAL REPORTS: Scientific and technical information considered important, complete, and a lasting contribution to existing knowledge.

TECHNICAL NOTES: Information less broad in scope but nevertheless of importance as a contribution to existing knowledge.

TECHNICAL MEMORANDUMS: Information receiving limited distribution because of preliminary data, security classification, or other reasons.

CONTRACTOR REPORTS: Scientific and technical information generated under a NASA contract or grant and considered an important contribution to existing knowledge.

TECHNICAL TRANSLATIONS: Information published in a foreign language considered to merit NASA distribution in English.

SPECIAL PUBLICATIONS: Information derived from or of value to NASA activities. Publications include conference proceedings, monographs, data compilations, handbooks, sourcebooks, and special bibliographies.

TECHNOLOGY UTILIZATION PUBLICATIONS: Information on technology used by NASA that may be of particular interest in commercial and other non-aerospace applications. Publications include Tech Briefs, Technology Utilization Reports and Notes, and Technology Surveys.

Details on the availability of these publications may be obtained from:

SCIENTIFIC AND TECHNICAL INFORMATION DIVISION
NATIONAL AERONAUTICS AND SPACE ADMINISTRATION
Washington, D.C. 20546